Max-Planck-Institut für Kernphysik

Max-Planck Institute for Nuclear Physics

High-precision Penning-trap experiment **PENTATRAP**

Sergey Eliseev
Max-Planck-Institute for Nuclear Physics, Heidelberg

Physics of fundamental Symmetries and Interactions, PSI Villigen, 16-21 October 2022

Experiment PENTATRAP

Max-Planck Institute for Nuclear Physics (Heidelberg)
Division “Stored and Cooled Ions” (Prof. Blaum)

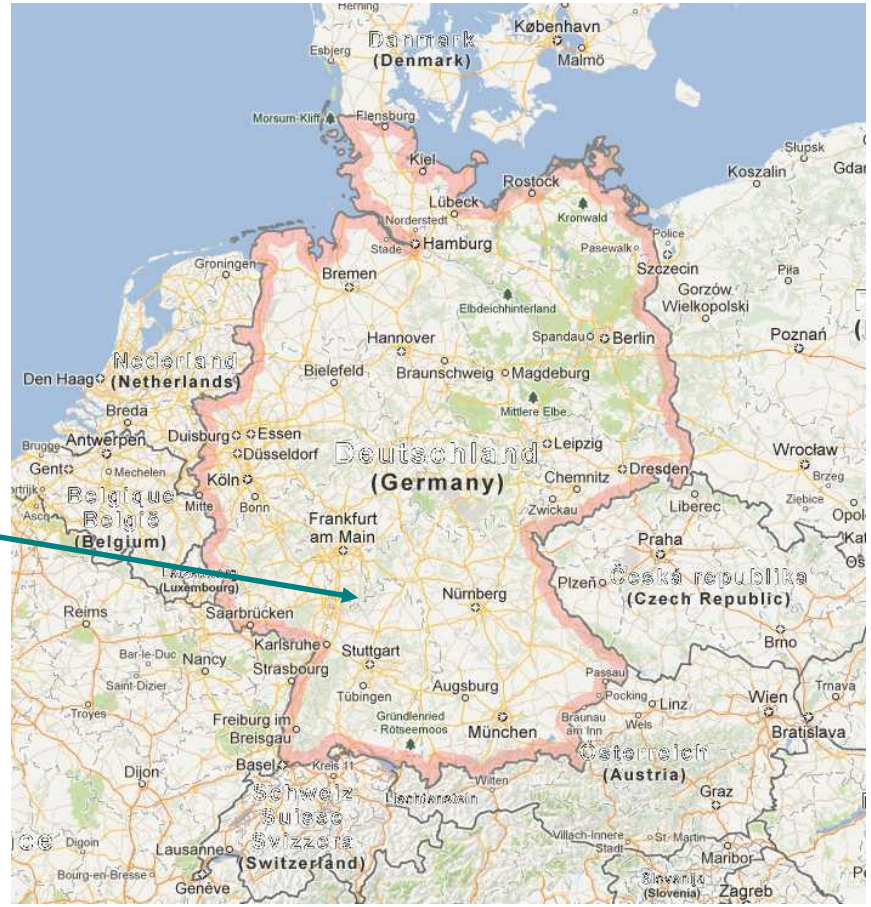

mass ratios of long-lived & stable nuclides
with an uncertainty **< 10^{-11}**

Precision of ***Mass-Ratio*** Measurements

Field	Examples	$\frac{\delta(m_1/m_2)}{m_1/m_2}$
Nuclear structure physics	shell closures, shell quenching, regions of deformation, drip lines, halos, S_n, S_p, S_{2n}, S_{2p}, δV_{pn}, island of stability	10^{-6} to 10^{-7}
Astrophysics nuclear models mass formula	*rp*-process and *r*-process path, waiting-point nuclei, proton threshold energies, astrophysical reaction rates, neutron star, x-ray burst	
Weak interaction studies	CVC hypothesis, CKM matrix unitarity, *Ft* of superallowed *ß*-emitters	10^{-8}
Metrology, fundamental constants	α (h/m_{Cs}, m_{Cs}/m_p, m_p/m_e), m_{Si}	10^{-9} to 10^{-10}
Neutrino physics	$m_{mother} - m_{daughter}$: $0\nu\beta\beta$, $0\nu 2EC$ sterile neutrinos neutrino mass	10^{-8}-10^{-9} $<10^{-11}$
metastable states 5th force, QED in HCI	mass ratios of ¥b, Ca, Sr, Nd, Ba isotopes electron binding energies	$<10^{-11}$

high-precision Penning-trap mass spectrometry

PENTATRAP

High-Precision Penning Traps Worldwide

on-line Penning-trap facilities for experiments on exotic nuclides

off-line Penning-trap setups for experiments on stable nuclides

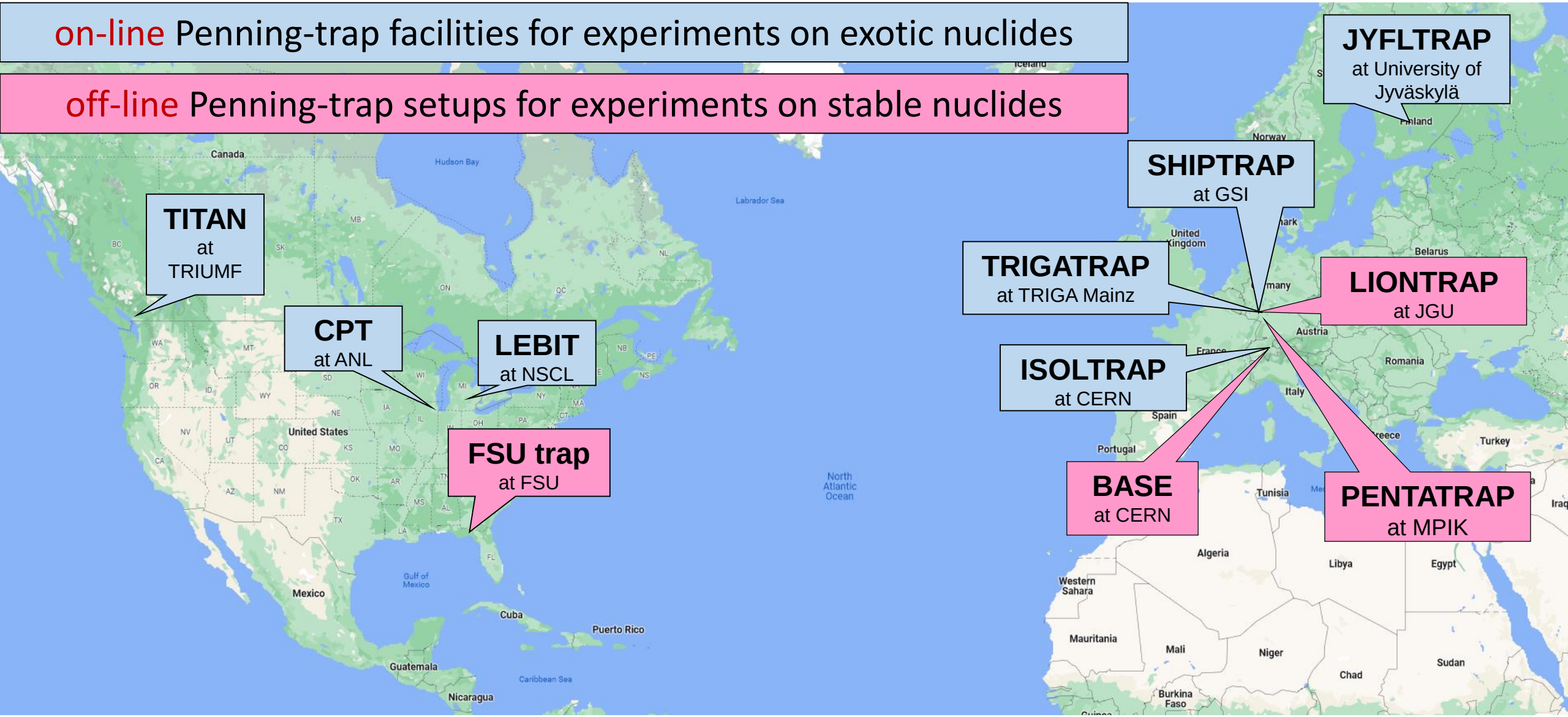

High-Precision Penning Traps Worldwide

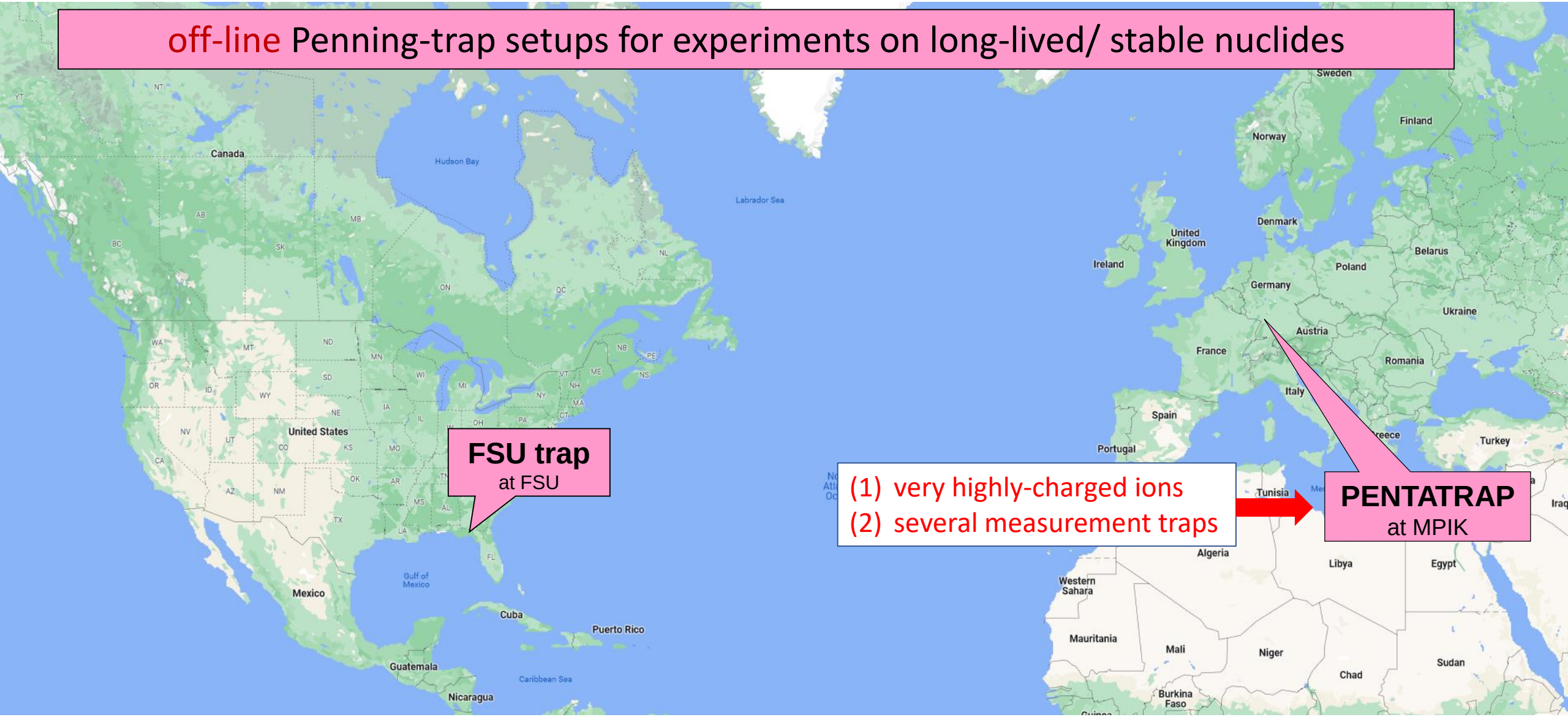

Penning Trap

strong uniform magnetic field

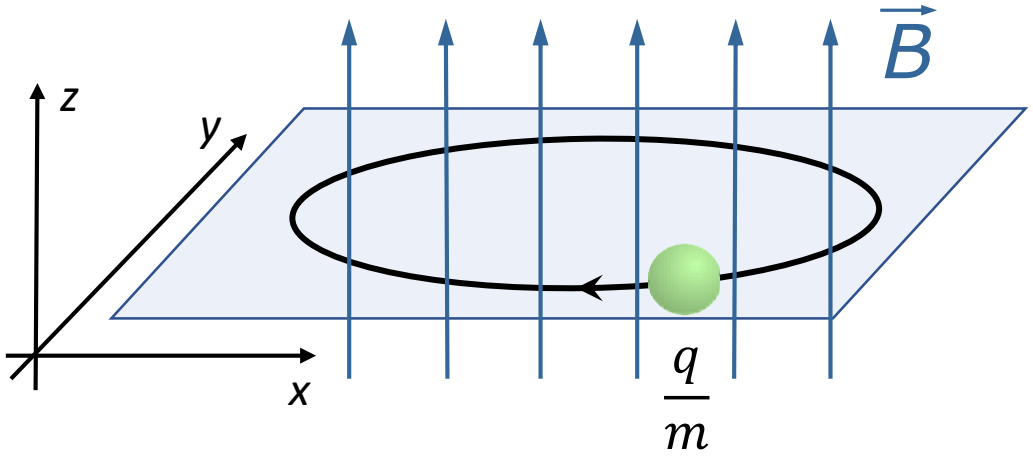

+

harmonic electrostatic potential

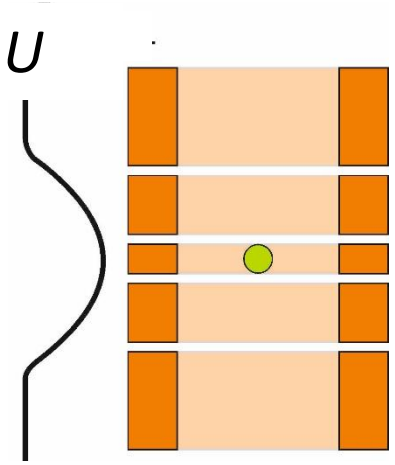

=

3 eigenmotions in trap

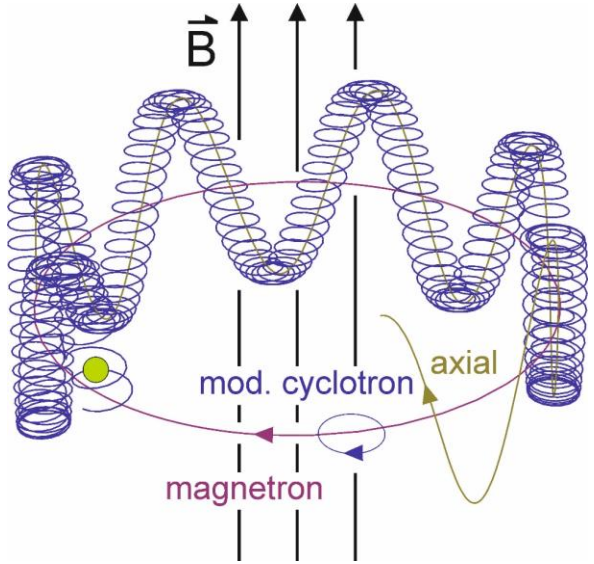

cyclotron motion: $\nu_+ = \nu_c \cdot \left(\frac{1}{2} + \frac{1}{2}\sqrt{1 - 2\nu_z^2}\right)$

axial motion: $\nu_z = \frac{1}{2\pi}\sqrt{\frac{q}{m} \cdot \frac{U}{d^2}}$

magnetron motion: $\nu_- = \nu_c \cdot \left(\frac{1}{2} - \frac{1}{2}\sqrt{1 - 2\nu_z^2}\right)$

Penning Trap

strong uniform magnetic field

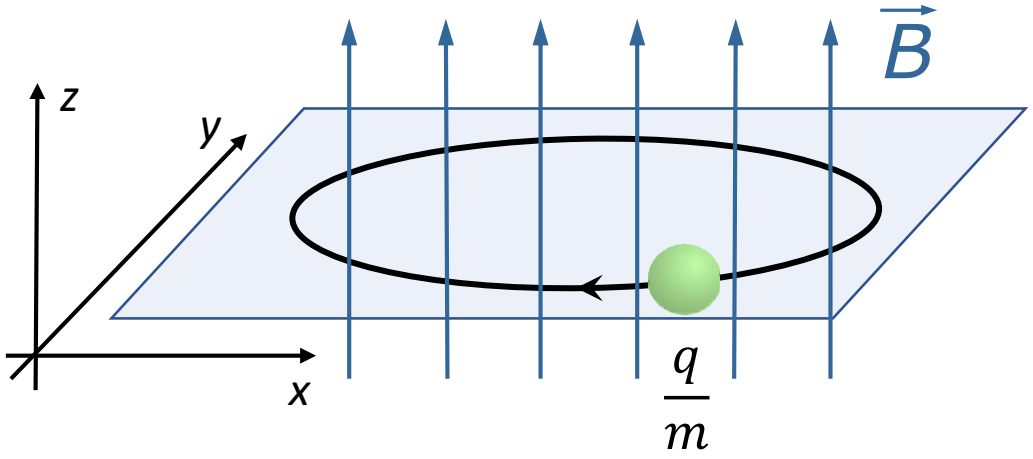

+

harmonic electrostatic potential

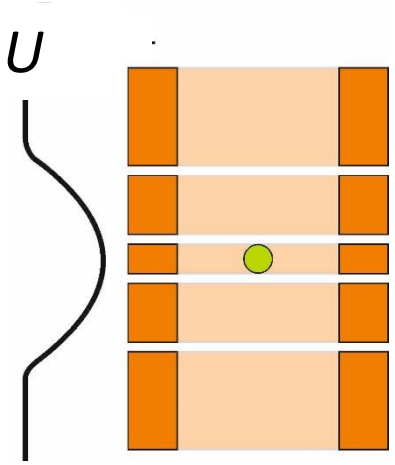

=

3 eigenmotions in trap

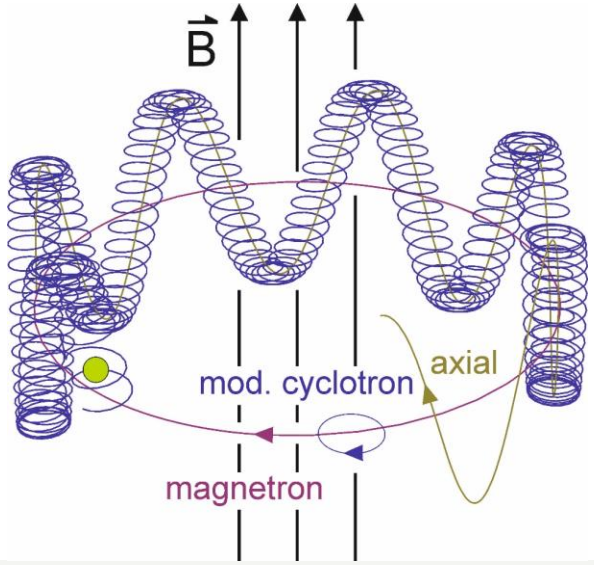

cyclotron frequency

$$\sqrt{\nu_+^2 + \nu_z^2 + \nu_-^2} = \nu_c = \frac{1}{2\pi}\frac{q}{m}B$$

L.S. Brown, G. Gabrielse, Phys. Rev. A 25 (1982) 2423.

$^{172}Yb^{42+}$

$\nu_+ \approx 26$ MHz	PnP technique
$\nu_z \approx 500$ kHz	dip technique
$\nu_- \approx 4$ kHz	double-dip technique

D. J. Wineland and H. G. Dehmelt, J. of Appl. Phys. 46 (1975) 919
E. A. Cornell *et al.*, Phys. Rev. Letter 63 (1989) 1674

PENTATRAP

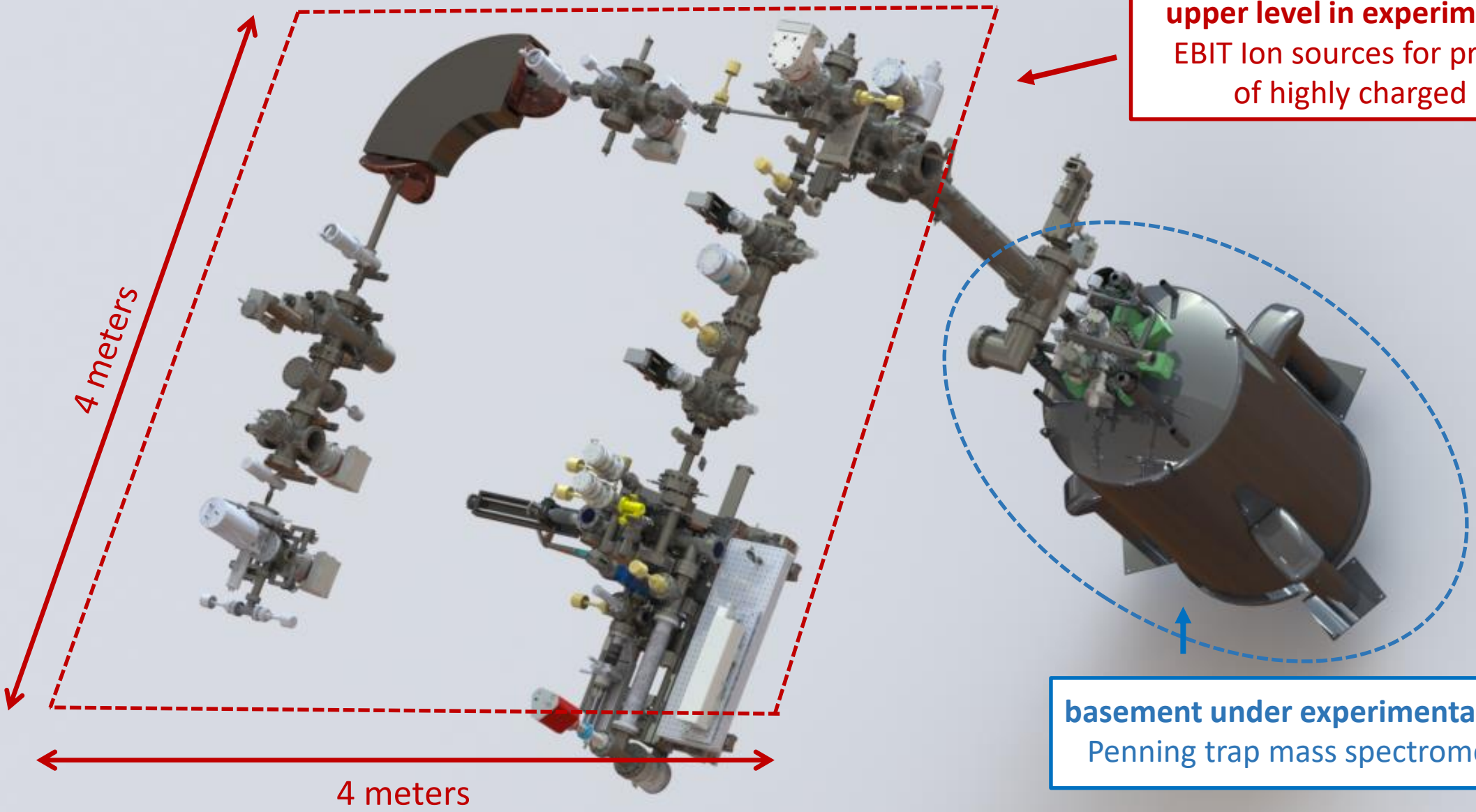

upper level in experimental hall:
EBIT Ion sources for production of highly charged ions

basement under experimental hall:
Penning trap mass spectrometer

PENTATRAP

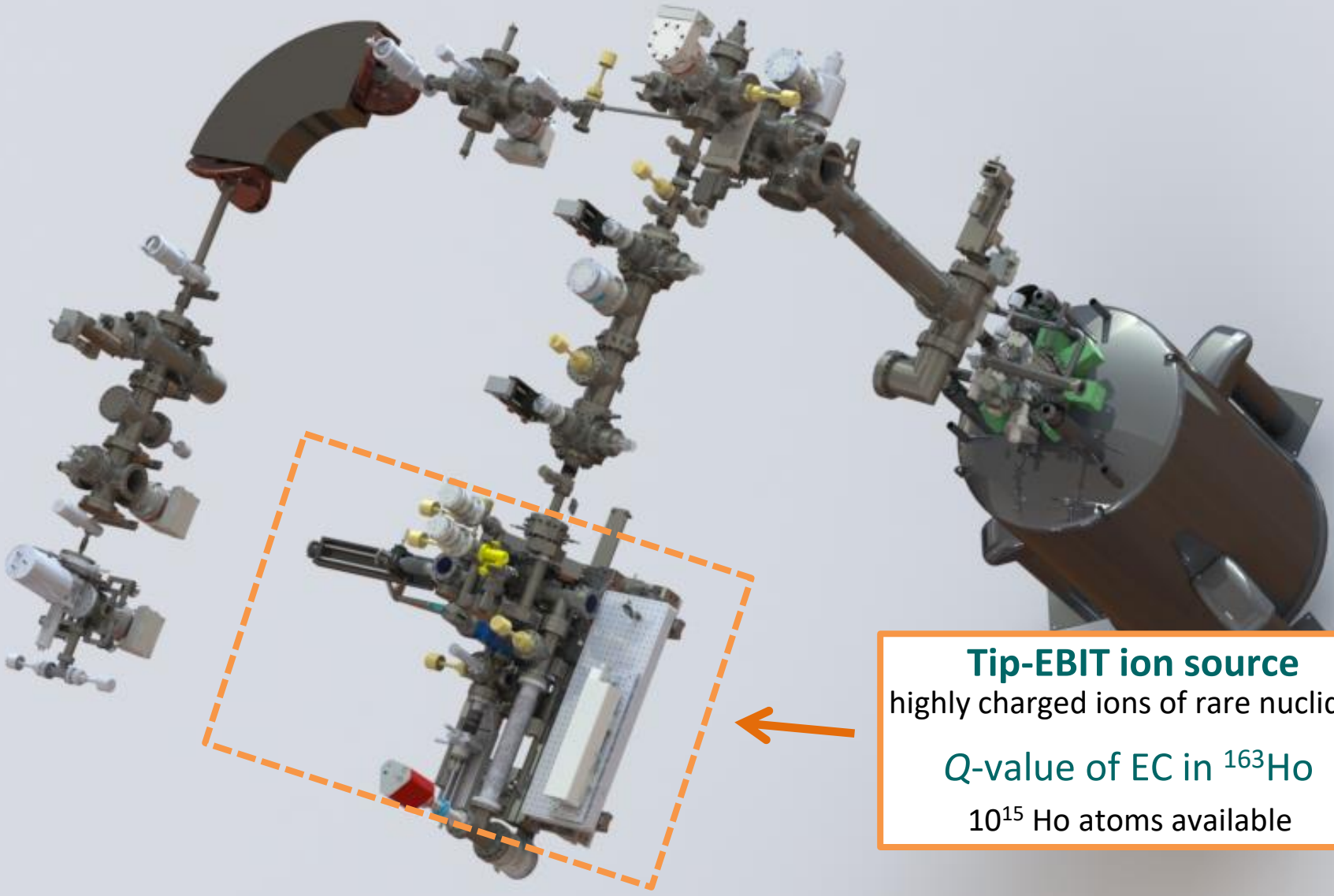

Tip-EBIT ion source
highly charged ions of rare nuclides

Q-value of EC in ^{163}Ho

10^{15} Ho atoms available

Tip-EBIT

Mini-EBIT developed in J.R. Crespo's group

Micke, P. et al., Rev. Sci. Instr. 89, 063109 (2018)

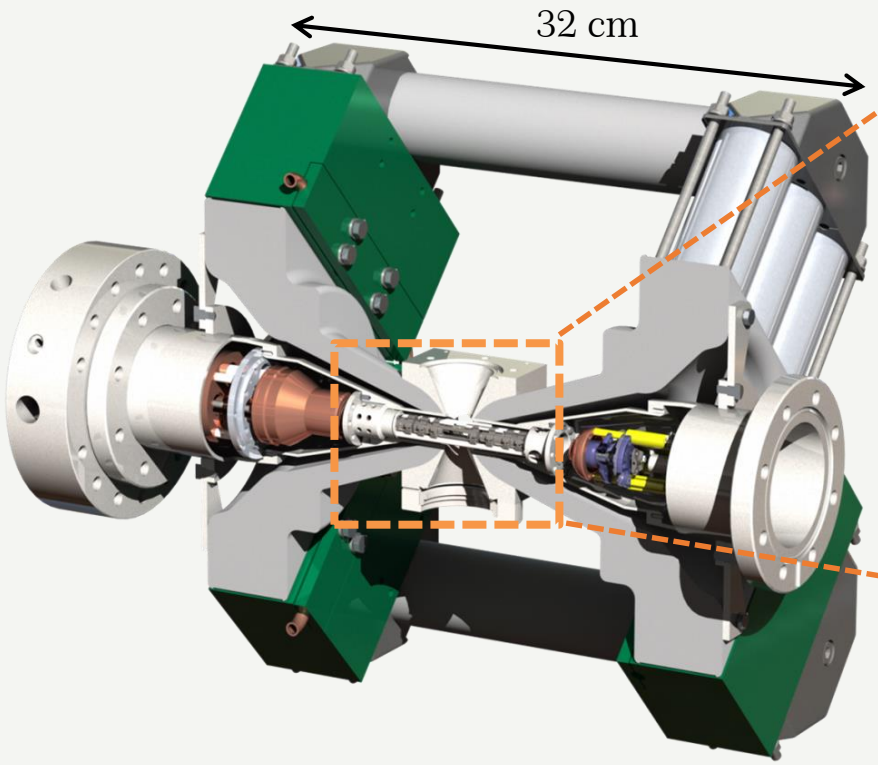

compact room temperature
permanent magnet, 0.85 T
max. electron current = 80 mA
max. electron energy = 10 keV

+

in-trap laser desorption

Schweiger, Ch. et al., Rev. Sci. Instr. 90, 123201 (2019)

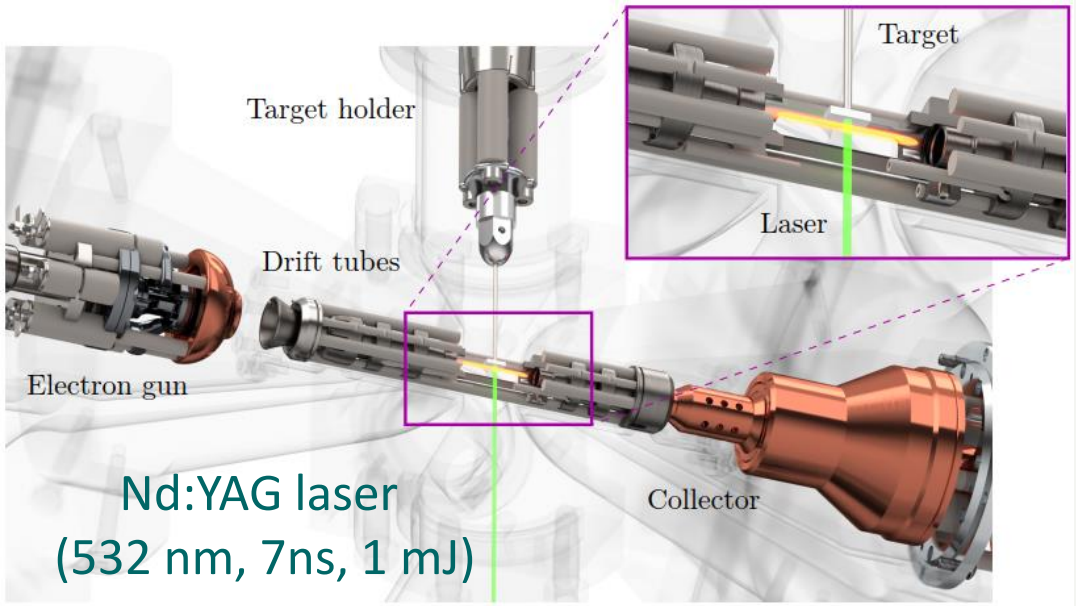

Nd:YAG laser
(532 nm, 7ns, 1 mJ)

^{165}Ho sample: 10^{12} atoms
life time: 20000 laser shots

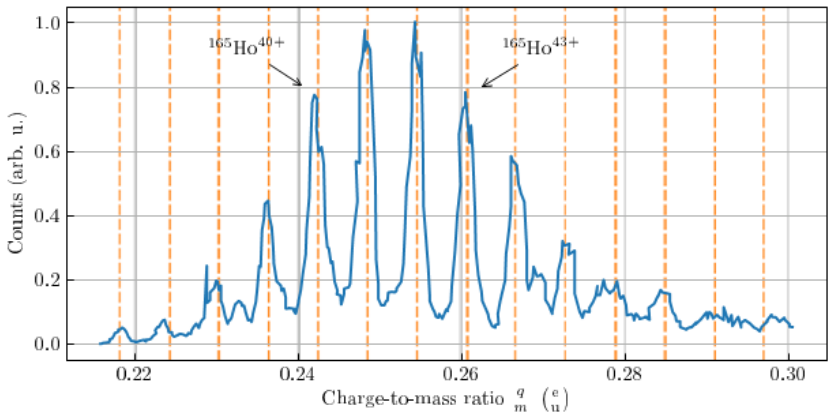

PENTATRAP

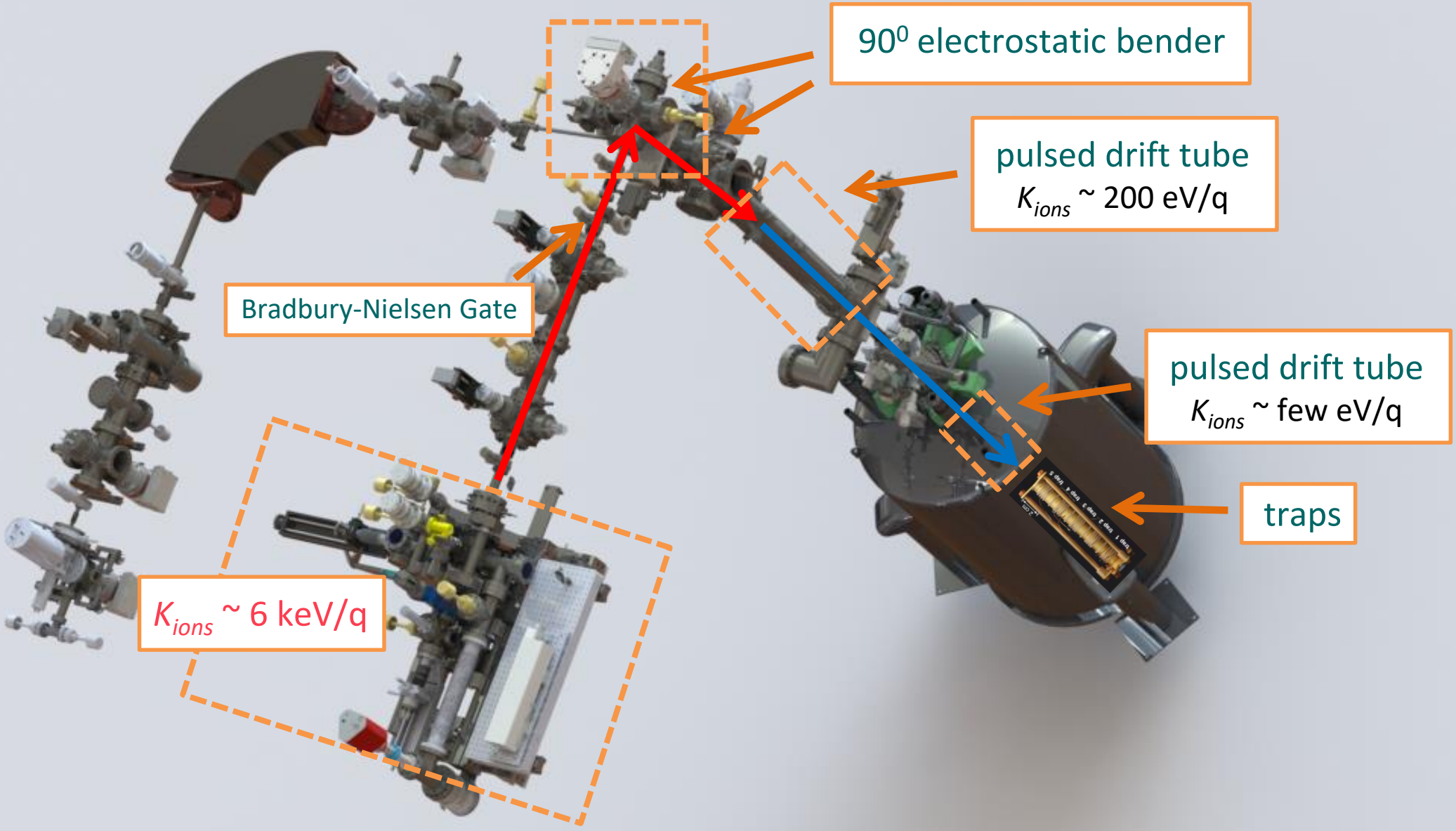
90⁰ electrostatic bender
pulsed drift tube
K_{ions} ~ 200 eV/q
Bradbury-Nielsen Gate
pulsed drift tube
K_{ions} ~ few eV/q
traps
K_{ions} ~ 6 keV/q

PENTATRAP

unique features of PENTATRAP:

- Stack of five Penning traps
- Cryogenic environment (4.2 K)
- 7 T superconducting magnet with vertical ***cold*** bore
- Temperature in the lab is stabilized: ± 0.05 K/day
- LHe-level in the bore is stabilized: ± 50 μm
- He-pressure in the bore is stabilized: ± 2 μbar
- Relative stability of *B*-field: 10^{-10} / hour
- Ultra-stable voltage source: $\Delta U/U < 10^{-7}$ / 100 s
- Highly charged ions

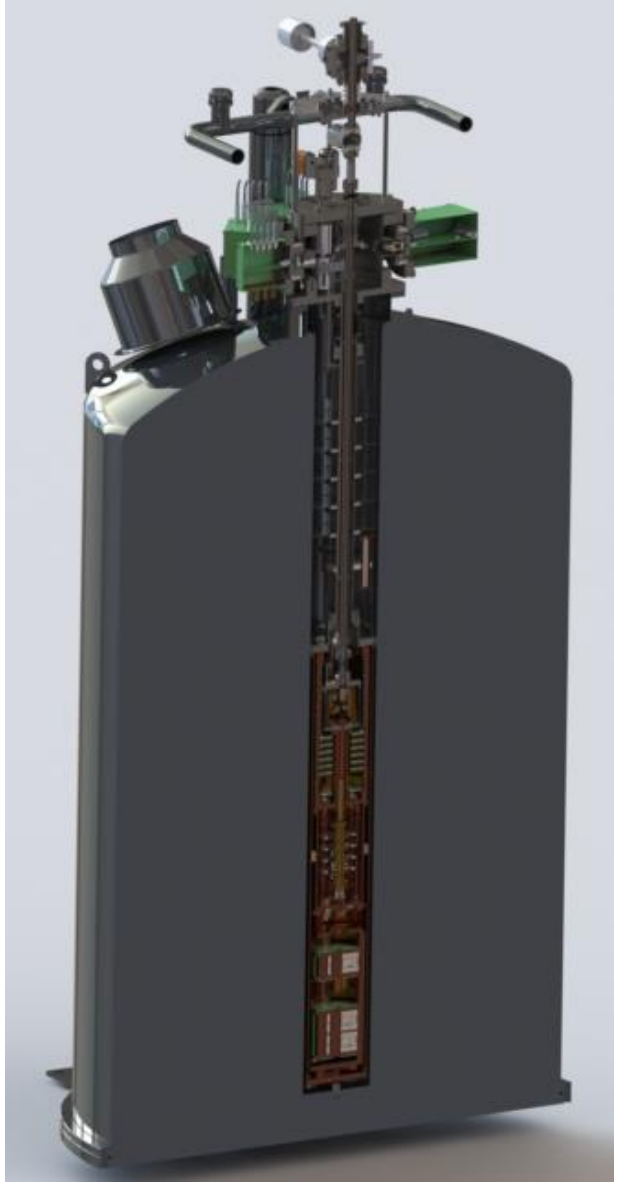

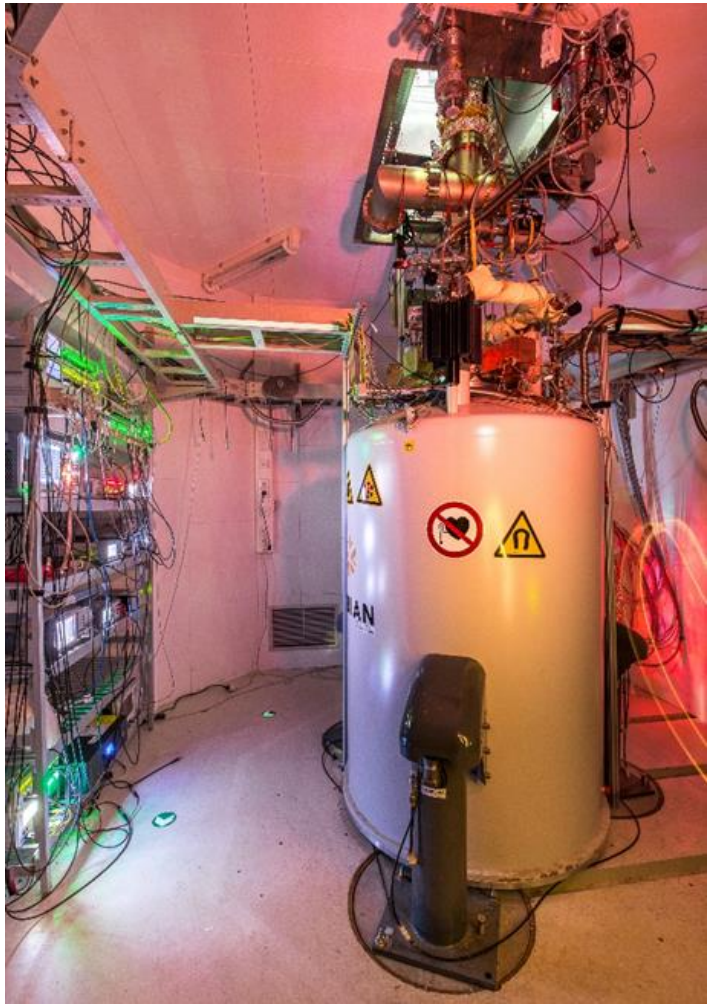

Repp, J. et al., Appl. Phys. B 107, 983 (2012)
Roux, C. et al., Appl. Phys. B 107, 997 (2012)
Böhm, C. et al., Nucl. Instrum. Meth. A 828, 125 (2016)

Measurement of trap frequencies with PENTATRAP

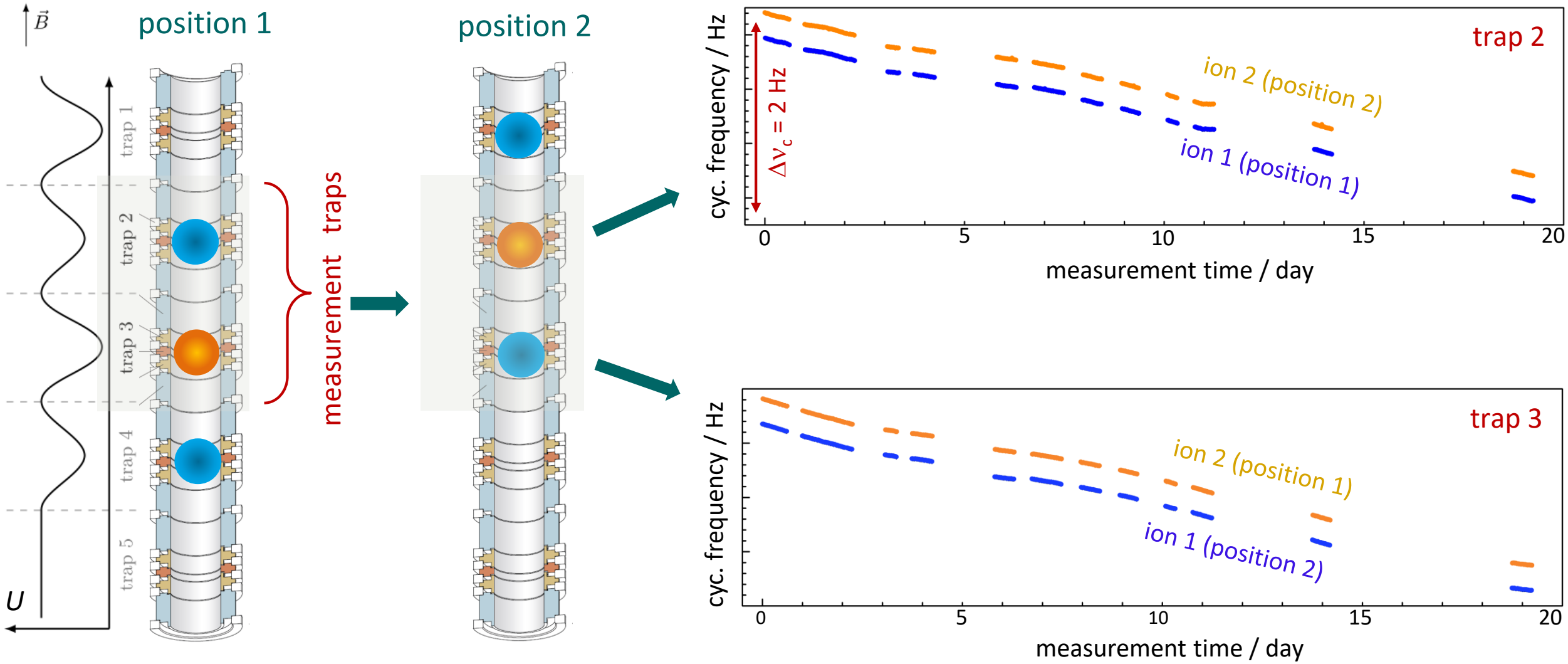

Measurement of trap frequencies with PENTATRAP

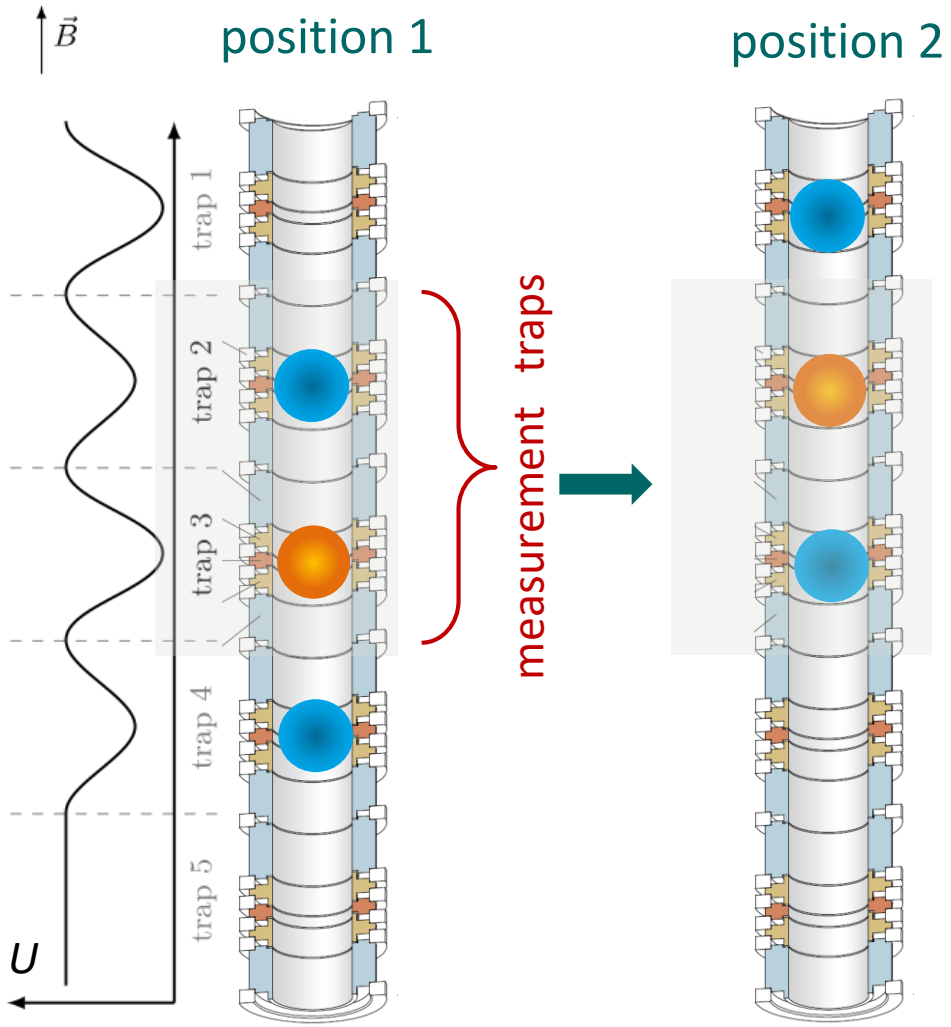

various data analysis methods:

- interpolation
- polynomial
- cancelation
- polycancel

reliability of results

Physics at PENTATRAP

neutrino mass:	$^{187}Re \rightarrow {}^{187}Os + e^- + \nu_e + Q_\beta$ $^{163}Ho + e^- \rightarrow {}^{163}Dy + \nu_e + Q_{EC}$
excitation energies of atomic metastable states:	$M(^{m}Re^{29+}) - M(Re^{29+})$ $M(^{m}Os^{30+}) - M(Os^{30+})$
test of QED in strong electromagnetic fields:	$M(^{20}Ne^{10+})$ vs $M(^{12}C^{6+})$
dark matter and 5th force:	chains of even isotopes Yb, Sr, Ca

Physics at PENTATRAP

neutrino mass:	$^{187}Re \rightarrow {}^{187}Os + e^- + \nu_e + Q_\beta$ $^{163}Ho + e^- \rightarrow {}^{163}Dy + \nu_e + Q_{EC}$
excitation energies of atomic metastable states:	$M(^{m}Re^{29+}) - M(Re^{29+})$ $M(^{m}Os^{30+}) - M(Os^{30+})$
test of QED in strong electromagnetic fields:	$M(^{20}Ne^{10+})$ vs $M(^{12}C^{6+})$
dark matter and 5th force:	chains of even isotopes Yb, Sr, Ca

Neutrino Mass

β^--decay of tritium

$$m_{\bar{\nu}_e} < 0.9 \frac{eV}{c^2} \; (90\% \; C.L.)$$

KATRIN experiment

The KATRIN Collaboration., Nature Phys. 18 (2022) 160.

$$Q_\beta = 18\,592.01(7) \; eV$$

FSU trap

E. G. Myers *et al.*, PRL 114 (2015) 013003.

β^--decay of ^{187}Re

MINEBA & MANU

$$m_{\bar{\nu}_e} < 15 \frac{eV}{c^2} \; (90\% \; C.L.)$$

M. Sisti et al., Nucl. Inst. Meth. A520, 125 (2004).

$$Q_\beta = 2466.7(1.6) \; eV$$

C. Arnaboldi et al., PRL 91, 161802 (2003).

$$Q_\beta = 2492(33) \; eV$$

SHIPTRAP D. Nesterenko et al., PRC 90, 042501 (R) (2014).

electron capture (EC) in ^{163}Ho

$$m_{\nu_e} < 225 \frac{eV}{c^2} \; (95\% \; C.L.)$$

P. Springer et al., Phys. Rev. A 35, 679 (1987).

$$Q_{EC} = 2858 \; (51) \; eV$$

ECHo P. Ranitzsch *et al.*, PRL 119, 122501 (2017).

$$Q_{EC} = 2833 \; (33) \; eV$$

SHIPTRAP S. Eliseev et al., PRL 115, 062501 (2015).

PENTATRAP for Neutrino Mass

β^--decay of ^{187}Re

MINEBA & MANU

$$Q_\beta = 2466.7(1.6)\ eV\ !!!$$

C. Arnaboldi et al., PRL 91, 161802 (2003).

Measurements 1: Q_{β_187Re} → mutial test of two techniques – PTMS & CM

Measurements 2: Q_{EC_163Ho} → determination of neutrino mass (ECHo experiment)

electron capture (EC) in ^{163}Ho

$$Q_{EC} = 2858\ (51)\ eV$$ ECHo P. Ranitzsch *et al.*, PRL 119, 122501 (2017).

$$Q_{EC} = 2833\ (33)\ eV$$ SHIPTRAP S. Eliseev et al., PRL 115, 062501 (2015).

Determination of Q-value of β^- -decay of ^{187}Re

^{187}Re: $T_{1/2} \approx 4 \cdot 10^{10}$ years; abundance ≈ 63%; a few mg of volatile $C_8H_5O_3Re$

^{187}Os: stable; abundance = 1.6%; a few mg of volatile $C_{10}H_{10}Os$

$$\frac{M[^{187}\mathrm{Re}] - M[^{187}\mathrm{Os}]}{M[^{187}\mathrm{Re}]} \approx 10^{-8} \text{ !!!}$$

we measure:

$$R = \frac{\nu_c[^{187}\mathrm{Os}^{29\,+}]}{\nu_c[^{187}\mathrm{Re}^{29\,+}]}$$

we want to determine:

$$Q = M[^{187}\mathrm{Re}] - M[^{187}\mathrm{Os}] = M[^{187}\mathrm{Os}^{29+}]\cdot[\boldsymbol{R}-1]+\boldsymbol{\Delta B}$$

optimal charge state for Re/Os ions is 29+:

- easy to achieve an uncertainty < 10^{-11} in R-measurement
- easy to produce 29+ Re/Os ions with our EBIT
- "easy" electron configurations: $^{187}Re^{29+}$ - $[Kr]4d^{10}$; $^{187}Os^{29+}$ - $[Kr]4d^{10}4f^{1}$

Maurits Haverkort
Heidelberg University Institute for Theoretical Physics

Zoltan Harman
Max-Planck Institute for Nuclear Physics

Paul Indelicato
Directeur de Recherche au CNRS

Determination of Q-value of β^- -decay of ^{187}Re

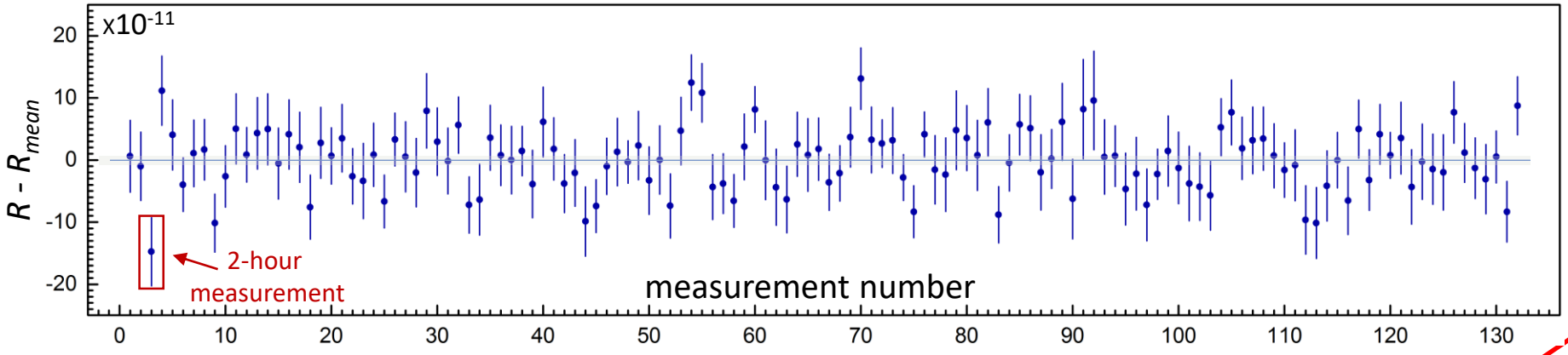

uncertainty in determination of ***R***

$5 \cdot 10^{-12}$

$$Q = M[^{187}\mathrm{Re}] - M[^{187}\mathrm{Os}] = M[^{187}\mathrm{Os}^{29+}]\cdot[\boldsymbol{R}-1]+\boldsymbol{\Delta B} = \mathbf{2470.9(1.3)\ eV}$$

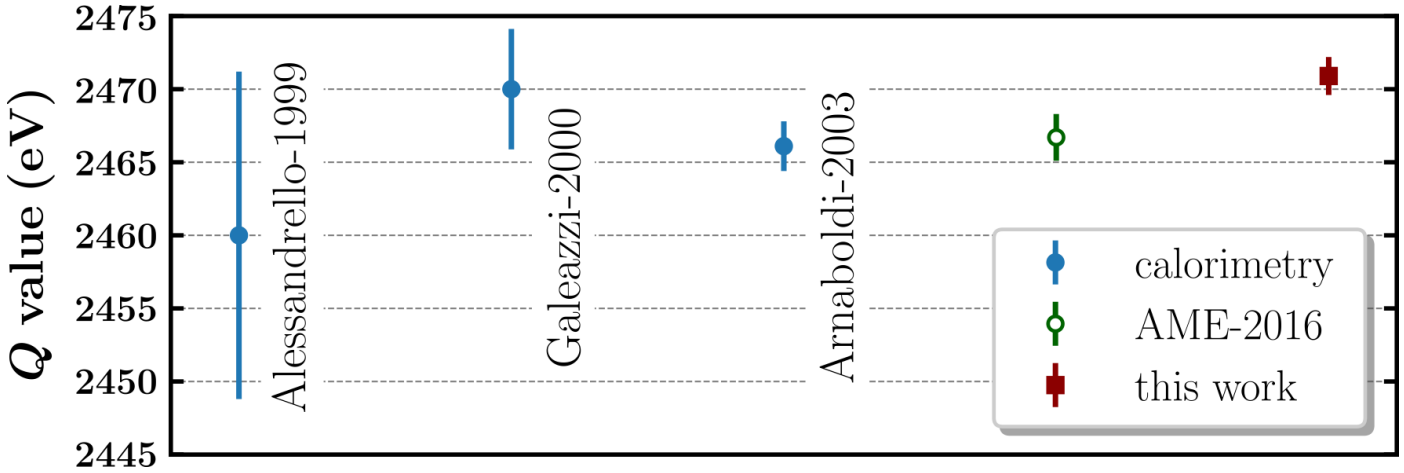

53.5(1.0) eV

Maurits Haverkort
Heidelberg University Institute for Theoretical Physics

Zoltan Harman
Max-Planck Institute for Nuclear Physics

Paul Indelicato
Directeur de Recherche au CNRS

PENTATRAP for Neutrino Mass

β^--decay of ^{187}Re

MINEBA & MANU

$$Q_\beta = 2466.7(1.6)\ eV\ !!!$$

C. Arnaboldi et al., PRL 91, 161802 (2003).

Measurements 1: $Q_{\beta\_187\mathrm{Re}}$ → mutial test of two techniques – PTMS & CM

Measurements 2: $Q_{EC\_163\mathrm{Ho}}$ → determination of neutrino mass (ECHo experiment)

electron capture (EC) in ^{163}Ho

$$Q_{EC} = 2858\ (51)\ eV$$ ECHo P. Ranitzsch *et al.*, PRL 119, 122501 (2017).

$$Q_{EC} = 2833\ (33)\ eV$$ SHIPTRAP S. Eliseev et al., PRL 115, 062501 (2015).

The Electron Capture in Holmium experiment

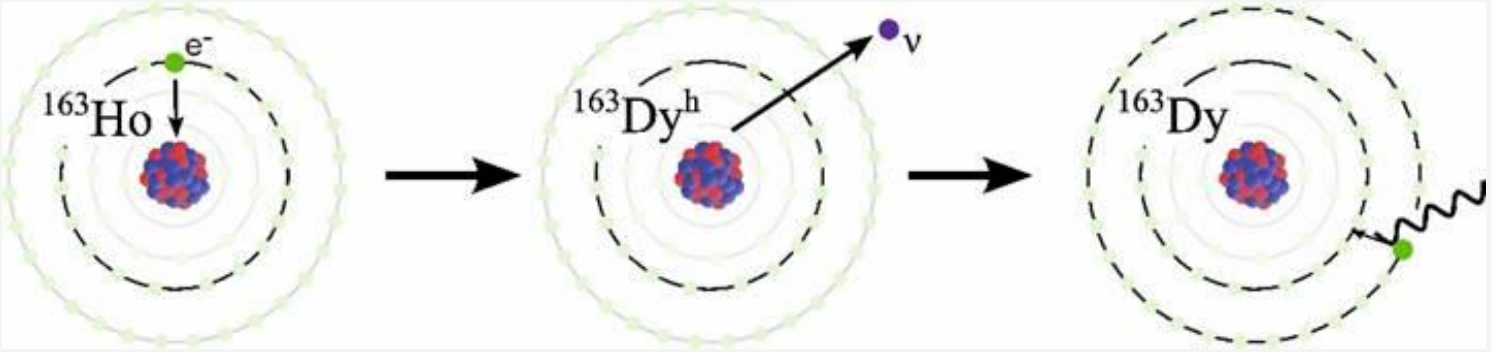

$$^{163}_{67}\mathrm{Ho} + e \rightarrow {}^{163}_{66}\mathrm{Dy}^{*} + \nu_e \rightarrow {}^{163}_{66}\mathrm{Dy} + E_c$$

$$\frac{dN}{dE} = F(Q, m_\nu)$$

M. Braß and M. W. Haverkort, arXiv: 2002.05989v1

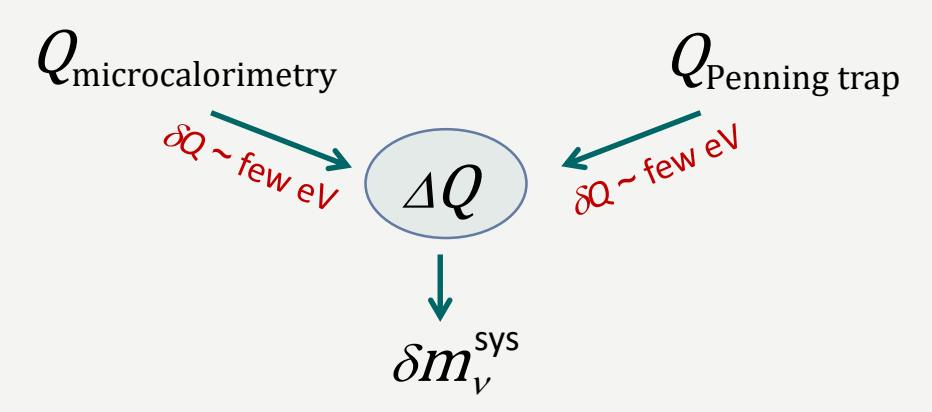

atomic de-excitation spectrum
(cryogenic microcalorimetry)

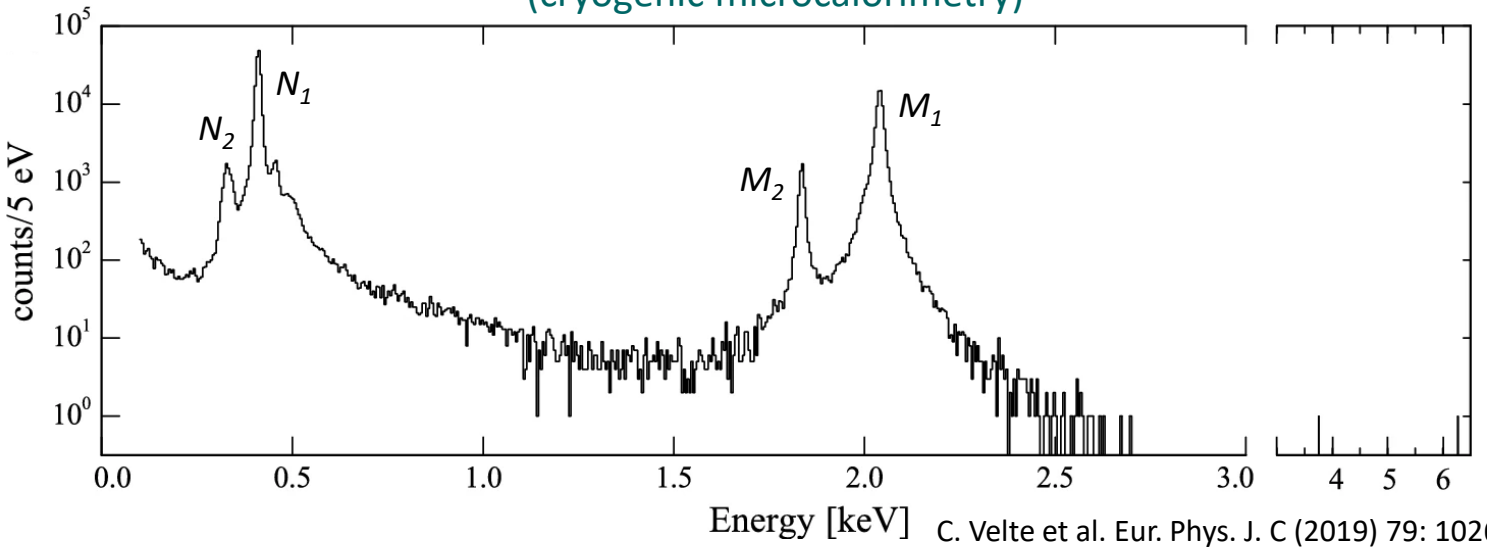

C. Velte et al. Eur. Phys. J. C (2019) 79: 1026

Determination of Q-value of EC in ^{163}Ho

$$Q = M[^{163}\mathrm{Ho}] - M[^{163}\mathrm{Dy}] = M[^{163}\mathrm{Dy}^{n+}]\cdot[\boldsymbol{R}-1]+\boldsymbol{\Delta B}$$

Maurits Haverkort
Zoltan Harman
Paul Indelicato

We have measured cyc-freq ratios of Dy and Ho in 3 charge states: 38+, 39+ and 40+

charge state	cyc freq ratio, *R*
38+	$1.0000000186233 \pm 3.0\cdot10^{-12}$
39+	$1.0000000113075 \pm 4.0\cdot10^{-12}$
40+	$1.0000000115156 \pm 3.5\cdot10^{-12}$

preliminary final uncertainty:

$$\delta Q < 0.8\ eV$$

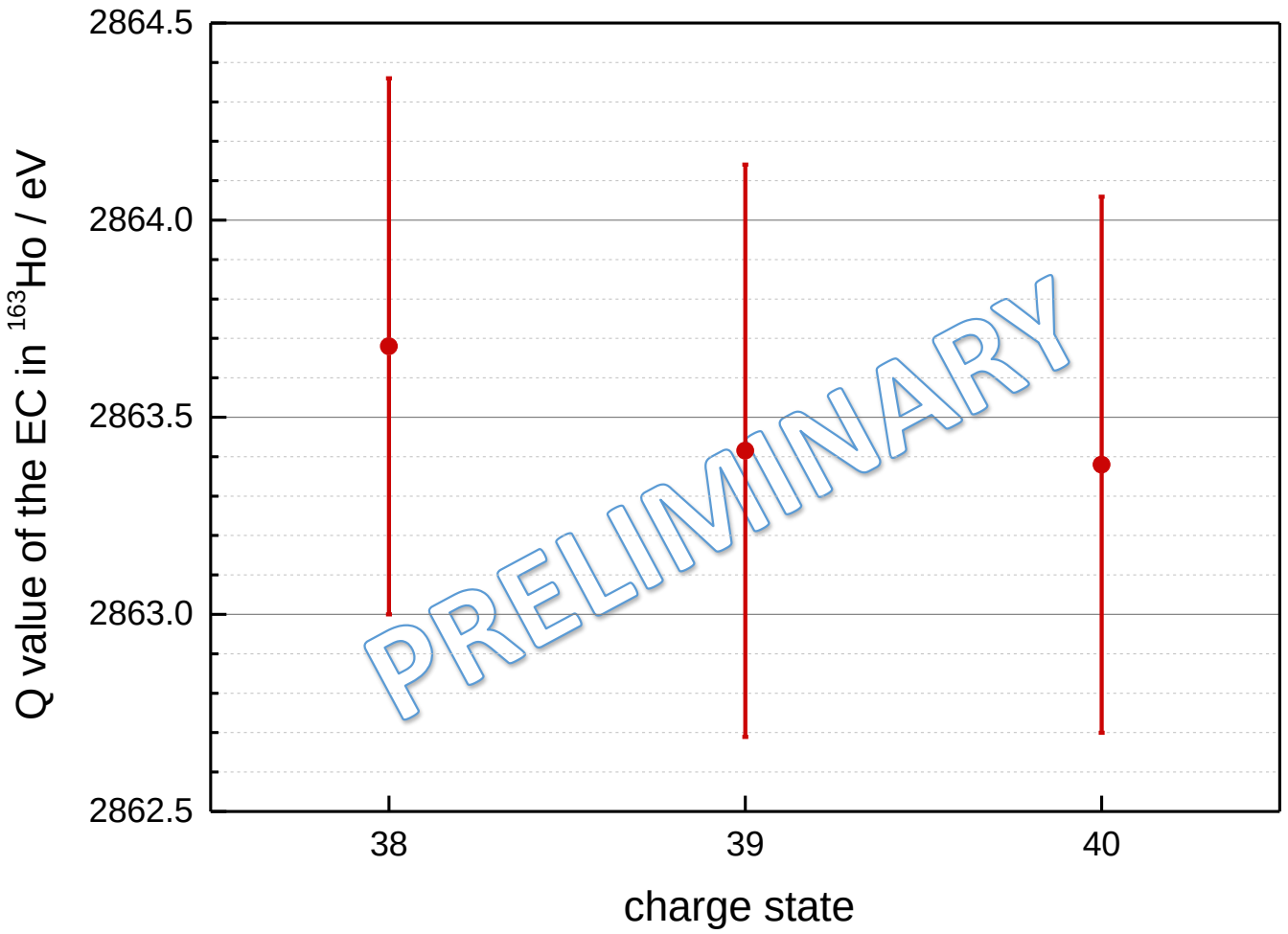

Physics at PENTATRAP

neutrino mass:	$^{187}Re \rightarrow {}^{187}Os + e^- + \nu_e + Q_\beta$ $^{163}Ho + e^- \rightarrow {}^{163}Dy + \nu_e + Q_{EC}$
excitation energies of atomic metastable states:	$M(^{m}Re^{29+}) - M(Re^{29+})$ $M(^{m}Os^{30+}) - M(Os^{30+})$
test of QED in strong electromagnetic fields:	$M(^{20}Ne^{10+})$ vs $M(^{12}C^{6+})$
dark matter and 5th force:	chains of even isotopes Yb,Nd, Ba, Sr, Ca

excitation energies of atomic metastable states

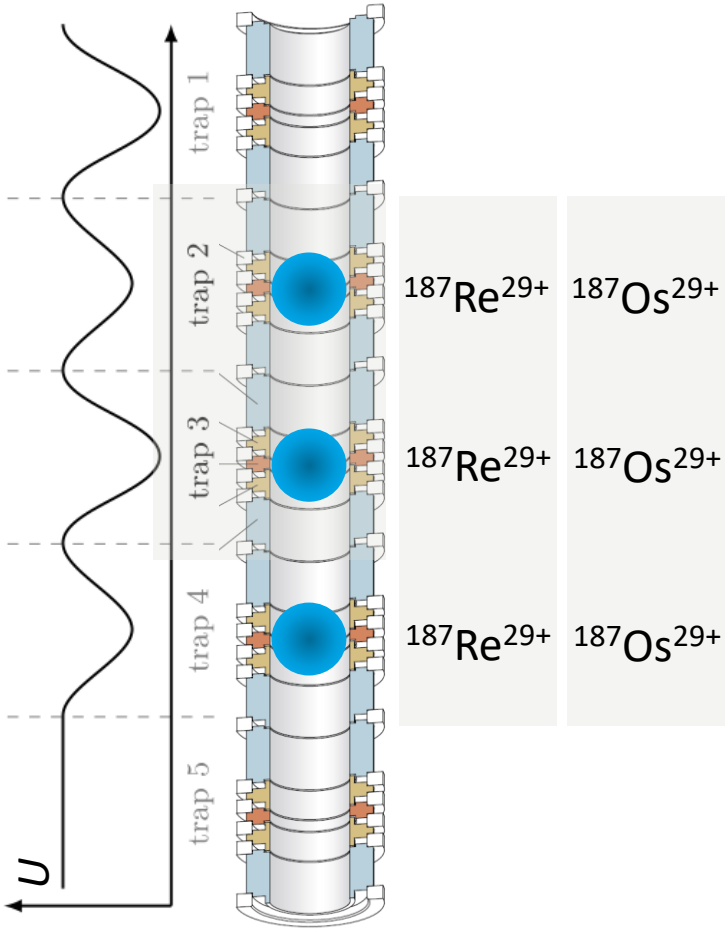

- Os^{29+} vs. Os^{29+} measurements yield always unity.
- Re^{29+} vs. Re^{29+} measurements yield either unity or $1+1.14\cdot10^{-9}$.

$^{187}Re^{29+}$

R. Schüssler et al., *Nature* 581, 42 (2020)

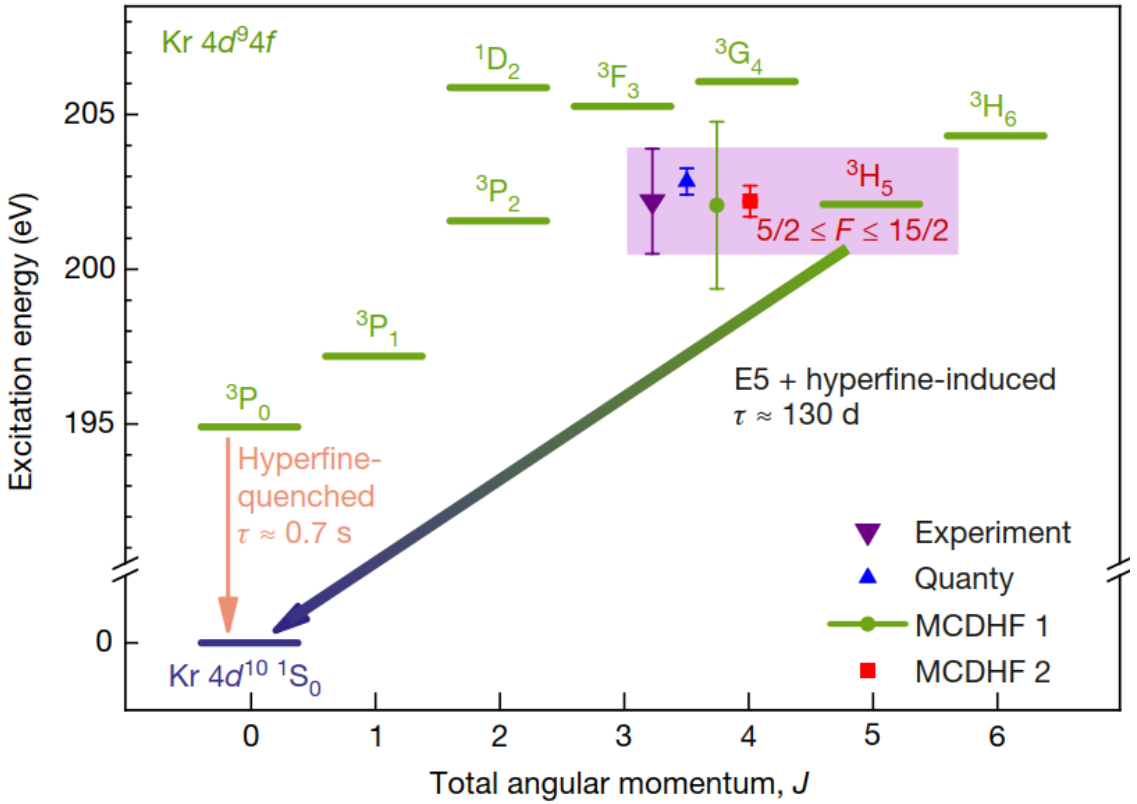

isoelectronic sequence:

Ta^{27+}, W^{28+}, **Re^{29+}**, Os^{30+}, Ir^{31+}, Pt^{32+}

excitation energies of atomic metastable states

Possible application: search for suitable clock transitions

Table 1. Summary of metastable state in highly charged ions.

isoelectron	ion	metastable state	energy (eV)	lifetime
23V-like	U^{69+}	$[Ar]3d^5\ {}^2H_{11/2}$	197.0	12.6 hours
23V-like	Th^{67+}	$[Ar]3d^5\ {}^2H_{11/2}$	176.3	25.3 hours
41Nb-like	U^{51+}	$[Kr]4d^5\ {}^2H_{11/2}$	57.5	8.3 days
22Ti-like	U^{70+}	$[Ar]3d^4\ {}^3H_4$	205.9	46.3 days
22Ti-like	Xe^{32+}	$[Ar]3d^4\ {}^5D_4$	17.9	3.0 hours
22Ti-like	Ba^{34+}	$[Ar]3d^4\ {}^5D_4$	21.1	10.3 hours
22Ti-like	Ce^{36+}	$[Ar]3d^4\ {}^5D_4$	24.8	54.5 hours
40Zr-like	U^{52+}	$[Kr]4d^5\ {}^2H_{11/2}$	59.8	10.9 years
40Zr-like	Gd^{24+}	$[Kr]3d^4\ {}^5D_4$	9.0	5.3 hours
40Zr-like	Dy^{26+}	$[Kr]3d^4\ {}^3F_4$	10.6	16.3 hours

next goal:

$$Xe^{32+}, Gd^{24+}, Dy^{26+}$$

Physics at PENTATRAP

neutrino mass:	$^{187}Re \rightarrow {}^{187}Os + e^- + \nu_e + Q_\beta$ $^{163}Ho + e^- \rightarrow {}^{163}Dy + \nu_e + Q_{EC}$
excitation energies of atomic metastable states:	$M(^{m}Re^{29+}) - M(Re^{29+})$ $M(^{m}Os^{30+}) - M(Os^{30+})$
test of QED in strong electromagnetic fields:	$M(^{20}Ne^{10+})$ vs $M(^{12}C^{6+})$
dark matter and 5th force:	chains of even isotopes Yb,Nd, Ba, Sr, Ca

Test of QED in strong electromagnetic fields

Measurement with Alphatrap of the g-factor of an electron in $^{20}Ne^{9+}$

$$g_{\mathrm{exp}} = 2 \frac{\nu_L}{\nu_c} \frac{m_e}{m\left({}^{20}_{10}Ne\right)} \frac{q}{e}$$

Alphatrap

from Atomic Mass Evaluation (AME)

Test of QED in strong electromagnetic fields

Measurement with Alphatrap of the g-factor of an electron in $^{20}Ne^{9+}$

$$g_{\mathrm{exp}} = 2\,\frac{\nu_L}{\nu_c}\,\frac{m_e}{m\left({}^{20}_{10}Ne\right)}\,\frac{q}{e}$$

Alphatrap

from Atomic Mass Evaluation (AME)

$$g_{\mathrm{exp}} \neq g_{\mathrm{theory}}$$

(discrepancy of about 3σ)

$^{20}Ne^{10+}$ vs $^{12}C^{6+}$

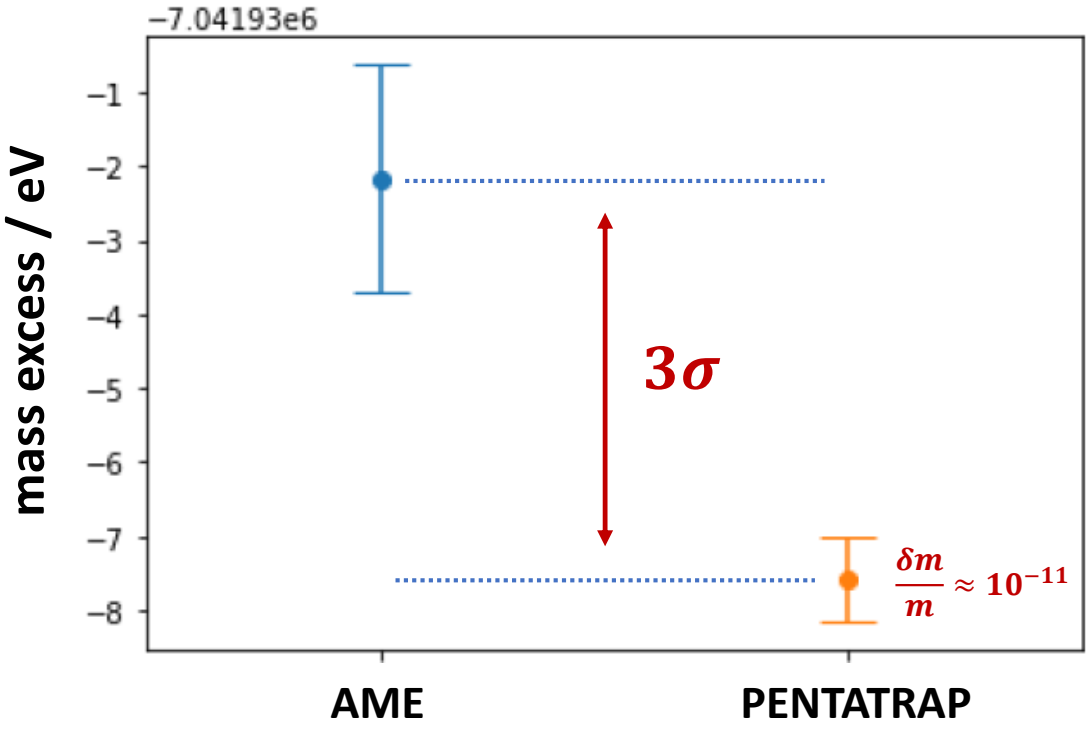

$$g_{\text{exp}} = g_{\text{theory}}$$

Physics at PENTATRAP

neutrino mass:	$^{187}Re \rightarrow {}^{187}Os + e^- + \nu_e + Q_\beta$ $^{163}Ho + e^- \rightarrow {}^{163}Dy + \nu_e + Q_{EC}$
excitation energies of atomic metastable states:	$M(^{m}Re^{29+}) - M(Re^{29+})$ $M(^{m}Os^{30+}) - M(Os^{30+})$
test of QED in strong electromagnetic fields:	$M(^{20}Ne^{10+})$ vs $M(^{12}C^{6+})$
dark matter and 5th force:	chains of even isotopes Yb, Sr, Ca

dark matter and 5th force

If Light Dark Matter particles exist: bosons, they couple quarks and leptons (5th force)

interraction of atomic electrons with a nucleus is altered,
atomic-electron binding energies & transition frequencies are changed

transition frequencies depend on nuclear mass

Penning traps

dark matter and 5th force

$$\Delta\nu_i = C_1 \cdot \frac{m_1 - m_2}{m_1 m_2} + C_2 \cdot \Delta\nu_j + \text{[higher−order SM effects + LDM bosons]}$$

$$\nu_i(\text{isotope}_1) - \nu_i(\text{isotope}_2) \equiv \Delta\nu_i$$

King plot

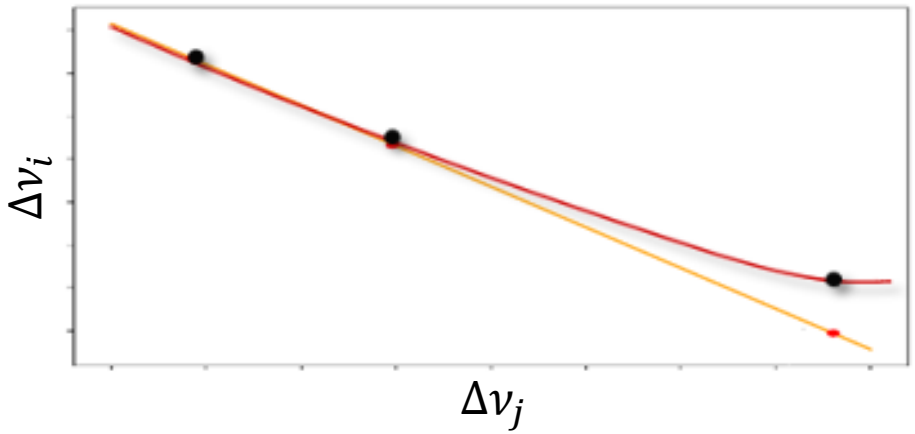

one needs elements with many even-even isotopes
and quadrupole/octupole (narrow optical) transitions:

^{168,170,172,174,176}Yb	I. Counts et al., PRL 125, 123002 (2020) K. Ono et al., arXiv: 2110.13544v2 J. Hur et al., arXiv: 2201.03578v2 N.L. Figueroa et al., PRL 128, 073001 (2022)
^{40,42,44,46,48}Ca	C. Solaro et al., PRL 125, 123003 (2020) F.W. Knollmann et al., PRA 100, 022514 (2019)
^{84,86,88,90}Sr	T. Manowitz et al., PRL 123, 203001 (2019) H. Miyake et al., PRR 1, 033113 (2019)

FUTURE:

$$\delta(\Delta\nu_i) \approx 10 \text{ mHz}$$

$$\delta\left(\frac{m_1}{m_2}\right) \approx 5 \cdot 10^{-12}$$

Yb mass-ratio measurements – ongoing !

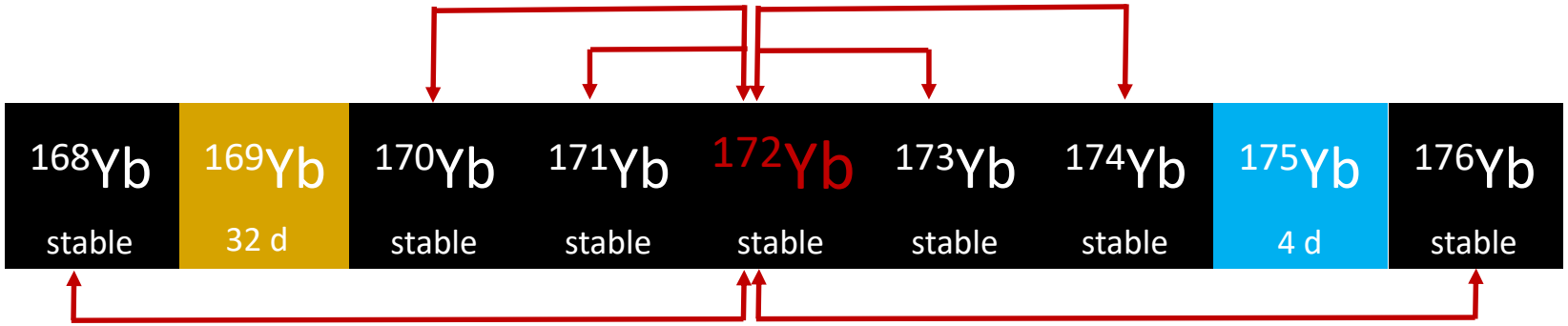

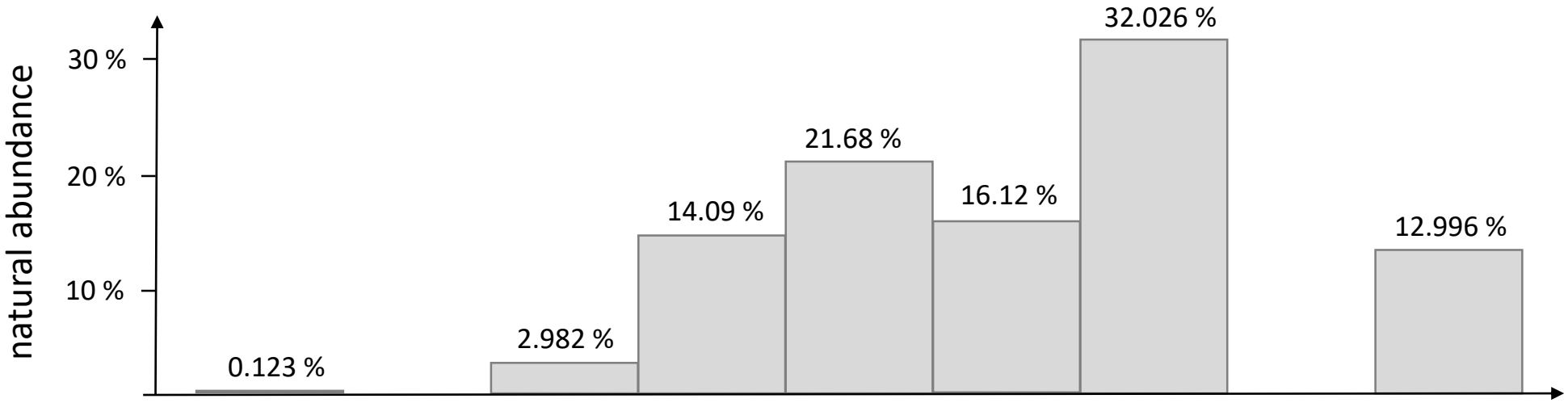

Yb mass-ratio measurements – ongoing !

cyclotron-frequency ratio of	statistical uncertainty
$^{172}Yb^{42+}$ / $^{168}Yb^{42+}$	$< 2\cdot10^{-12}$
$^{172}Yb^{42+}$ / $^{170}Yb^{42+}$	$< 2\cdot10^{-12}$
$^{172}Yb^{42+}$ / $^{171}Yb^{42+}$	
$^{172}Yb^{42+}$ / $^{173}Yb^{42+}$	
$^{172}Yb^{42+}$ / $^{174}Yb^{42+}$	$< 2\cdot10^{-12}$
$^{172}Yb^{42+}$ / $^{176}Yb^{42+}$	$< 2\cdot10^{-12}$

error budget	
statistics	$< 2\cdot10^{-12}$
relativistic shift	$\sim 2\cdot10^{-12}$
axial fit	$\sim 2\cdot10^{-12}$
binding energy	$< 10^{-12}$
total uncertainty $\sim 5 \cdot 10^{-12}$	

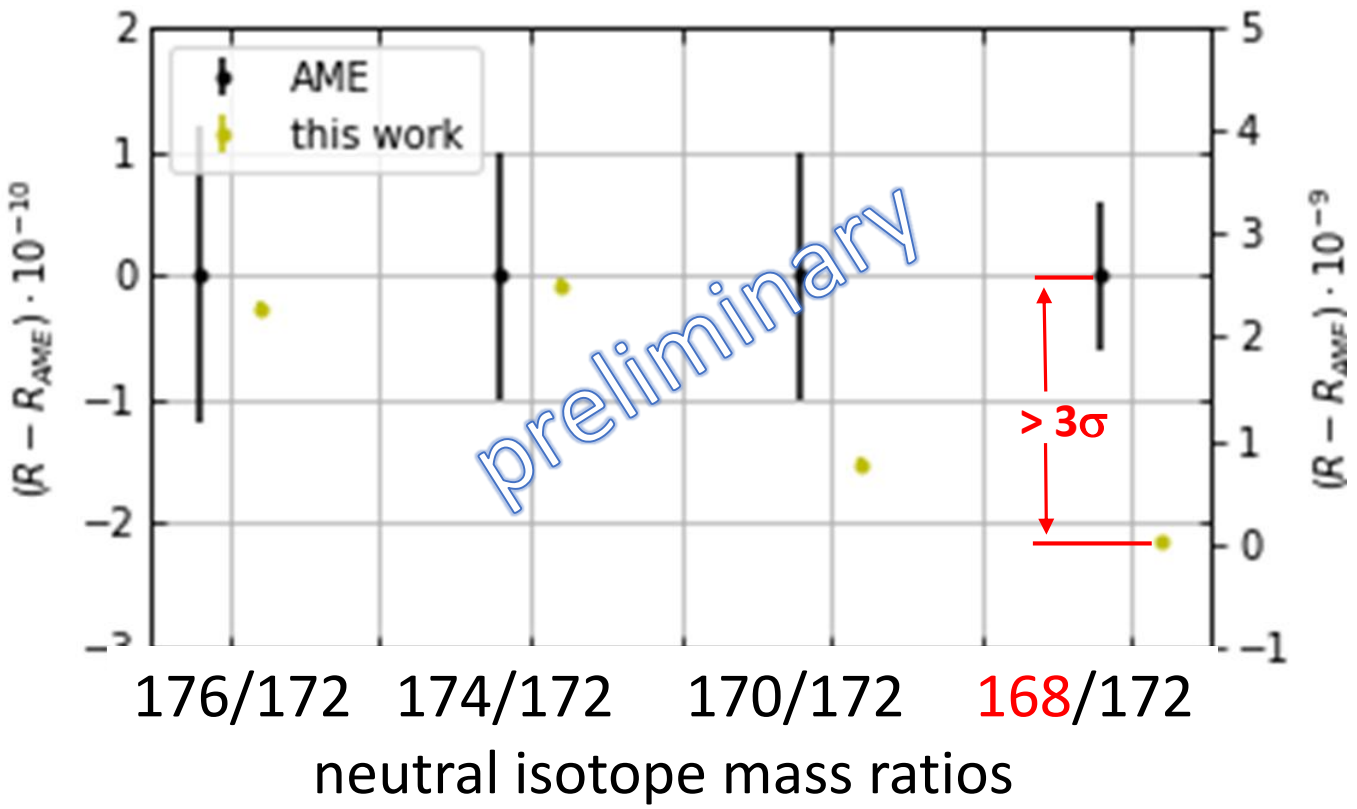

“near“ future measurements

- **Yb – isotopes** (dark matter): $\delta R \approx 5 \cdot 10^{-12}$
- **Ca – isotopes** (dark matter): $\delta R \approx 10^{-11}$
- $\mathbf{Xe^{32+}}$, $\mathbf{Gd^{24+}}$, $\mathbf{Dy^{26+}}$ (metastable states): $\delta R \approx 10^{-12}$
- ^{133}**Cs vs** ^{12}**C** (α-constant): $\delta R \approx 10^{-11}$

Max-Planck-Institut für Kernphysik

Max-Planck Institute for Nuclear Physics

Thank you for your attention!

DFG FOR 2202

DFG SFB 1225

ERC AdG 832848 - FunI

IMPRS-PTFS

Present and former PENTATRAP members:

Christine Böhm, Menno Door, Andreas Dörr, Sergey Eliseev, Pavel Filianin, Daniel Lange, Kathrin Kromer, Marius Müller, Yuri N. Novikov, Julia Repp, Alexander Rischka, Christian Roux, Christoph Schweiger, Rima X. Schüssler, and Klaus Blaum

Backup Slides

Data Analysis: Cancel Method

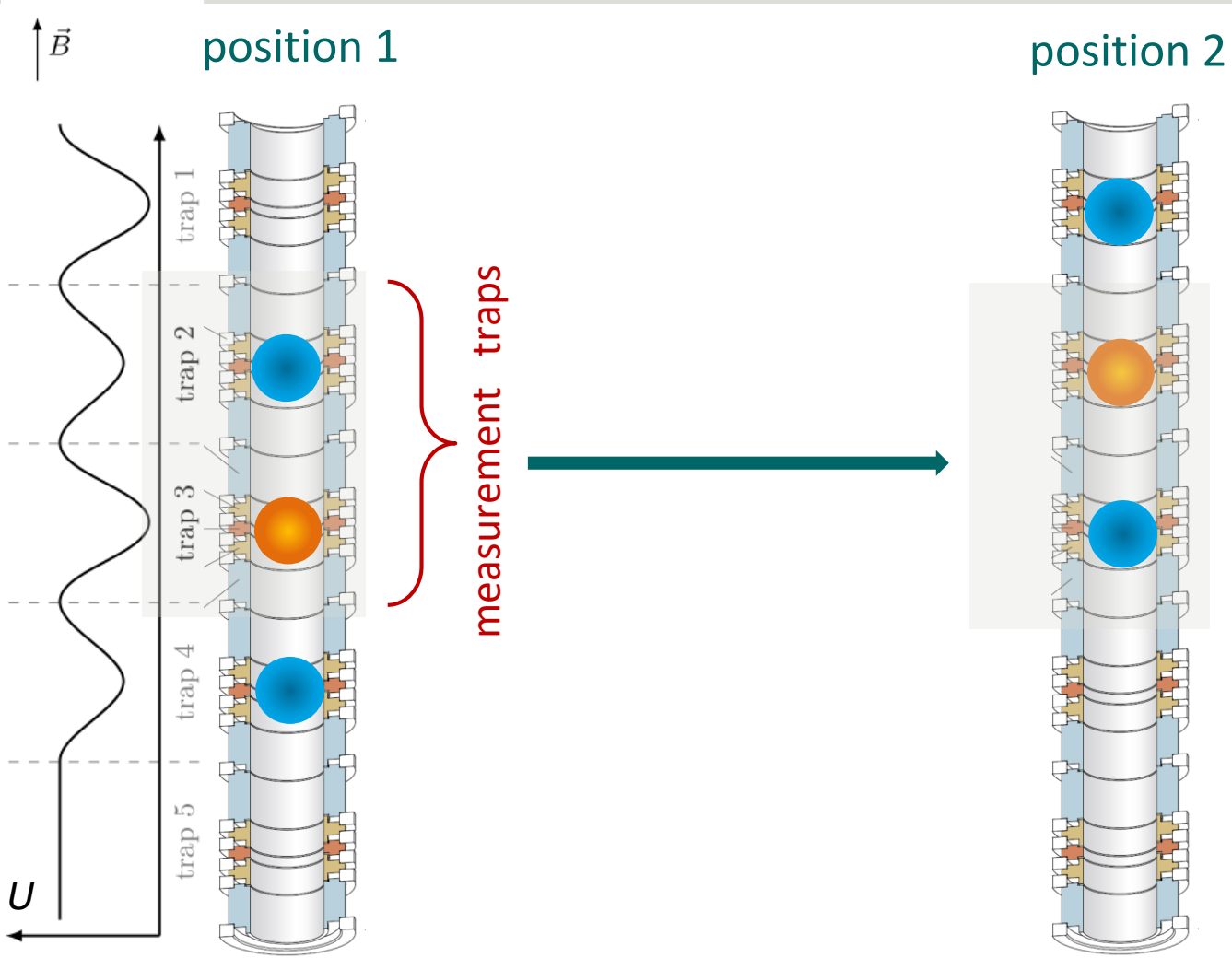

$$R = \sqrt{R(t_1)R(t_2)} = \frac{m_2}{m_1}$$

$$if\ \frac{B_{trap2}}{B_{trap3}} = const$$

$$R(t_1) = \frac{\nu_{ion1}}{\nu_{ion2}}(t_1) = \frac{m_2}{m_1}\frac{B_{trap2}}{B_{trap3}}(t_1)$$

$$R(t_2) = \frac{\nu_{ion1}}{\nu_{ion2}}(t_2) = \frac{m_2}{m_1}\frac{B_{trap3}}{B_{trap2}}(t_2)$$

Dresden-EBIT

compact room temperature
permanent magnet, 0.2 T
max. electron current = 30 mA
max. electron energy = 12 keV

gases & volatile chem. compounds
Ar, Xe, Re, Os…….
sample size ~ a few mg

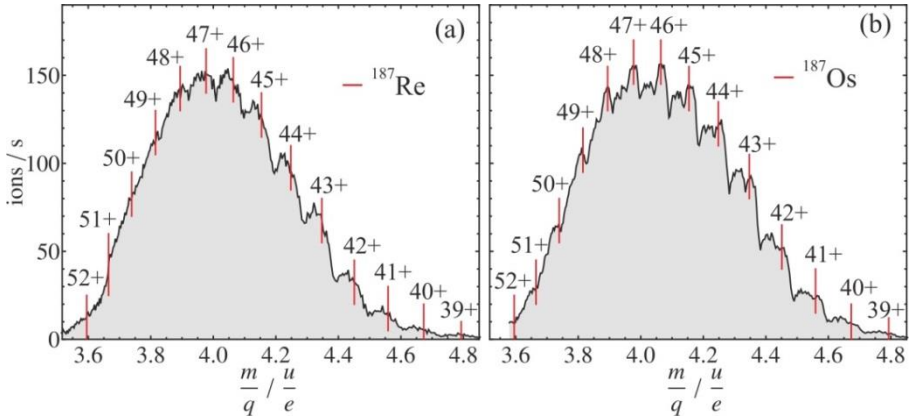

Dresden-EBIT

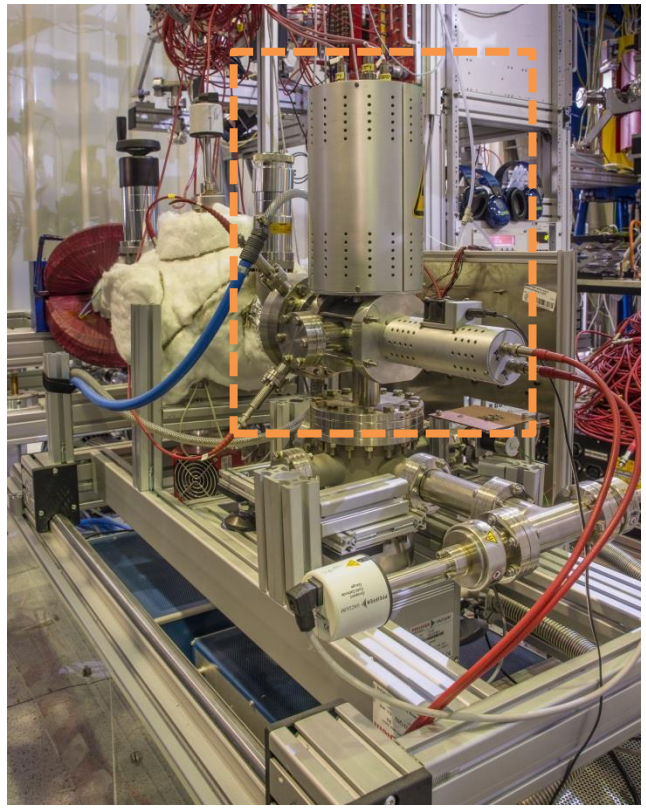

MIVOC inlet system

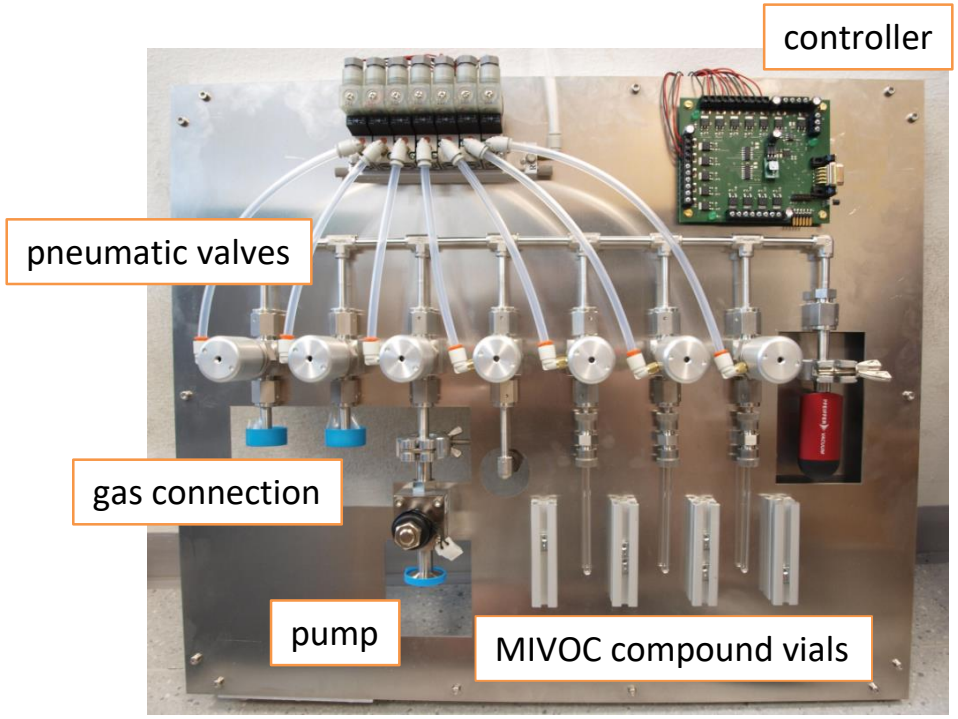

Tip - EBIT

Massive ^{165}Ho target

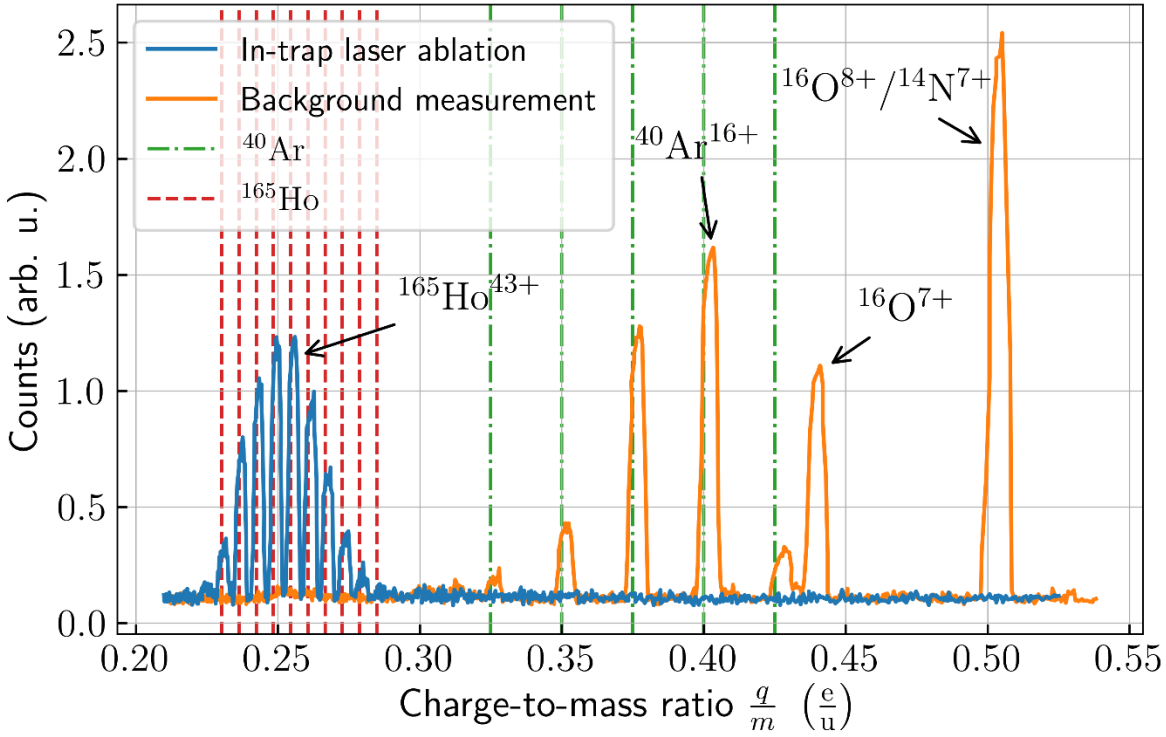

Blue curve: Laser ablation from ^{165}Ho target
Orange curve: Background measurement without laser

Tip - EBIT

Small holmium targets

- 1 mm diameter Ti-wire
- Targets with known number of ^{165}Ho atoms on the surface:

  Drop-on-demand inkjet printing technique (group of Ch. Düllmann @ JGU Mainz)

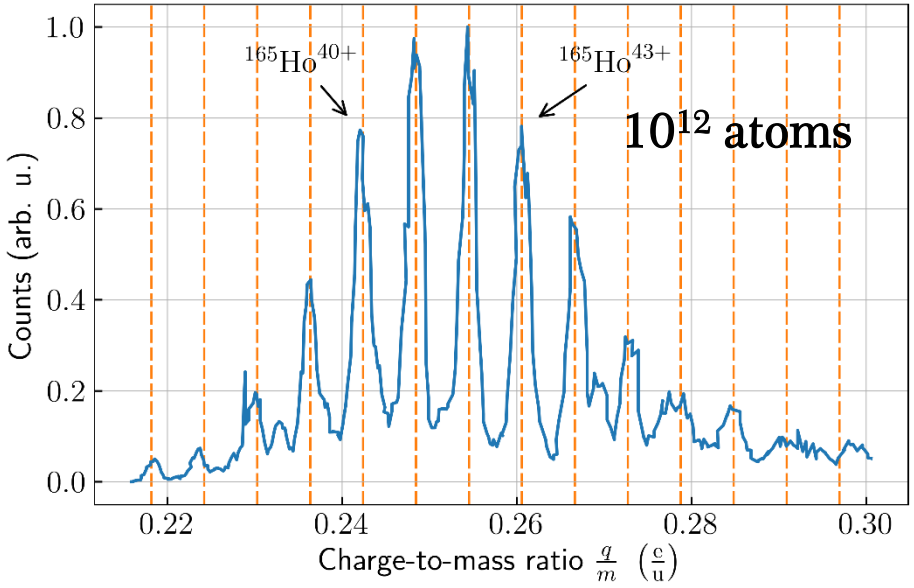

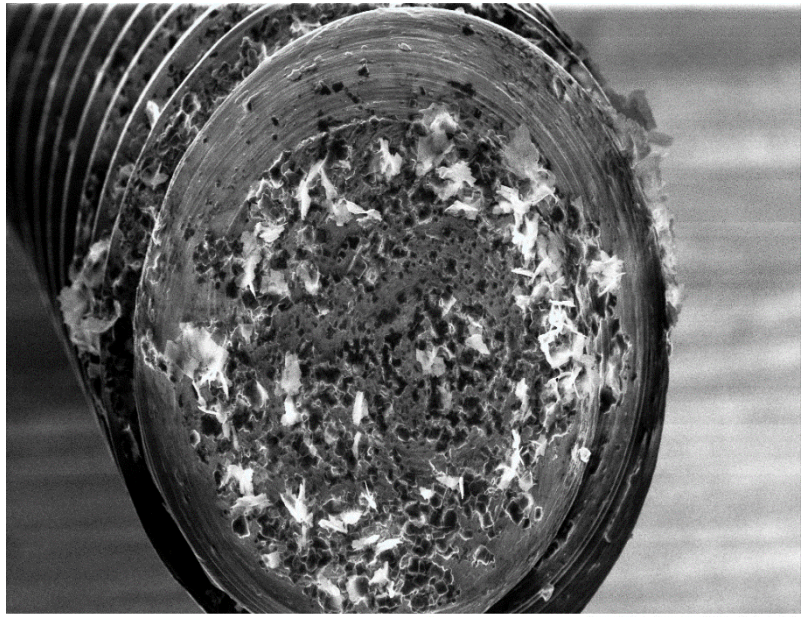

Tip - EBIT

Targets for in-trap laser desorption

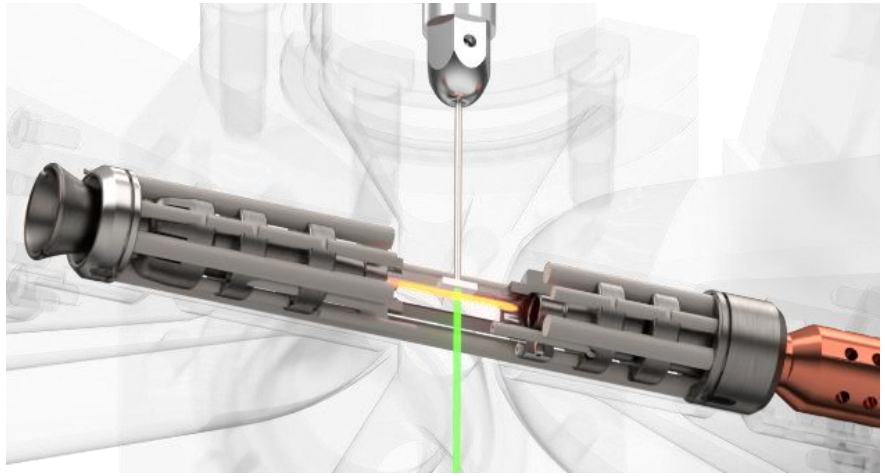

Target types:

- „Drop-on-demand“ printed targets: µg to ng samples, smallest target: 10^{12} atoms ^{165}Ho
- PLA-target: tens of µg to mg
- Massive targets: mg samples, e.g. metallic foil, bulk material

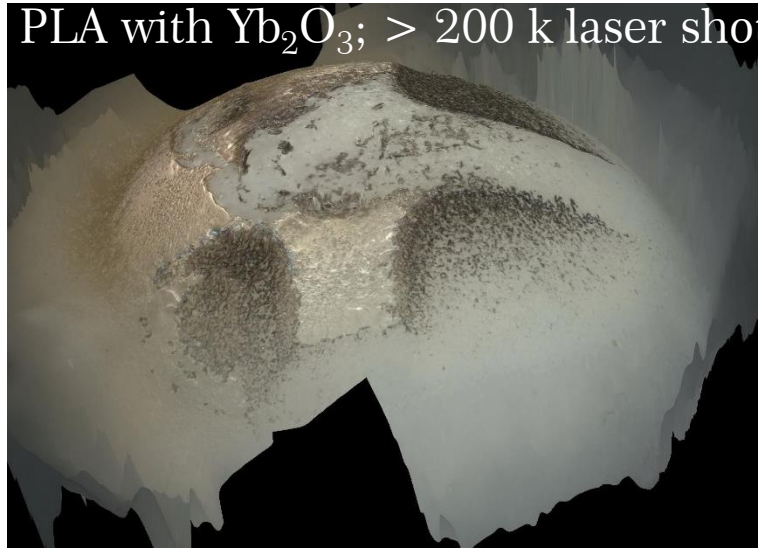

Determination of *Q*-value of EC in ^{163}Ho

in-trap laser desorption

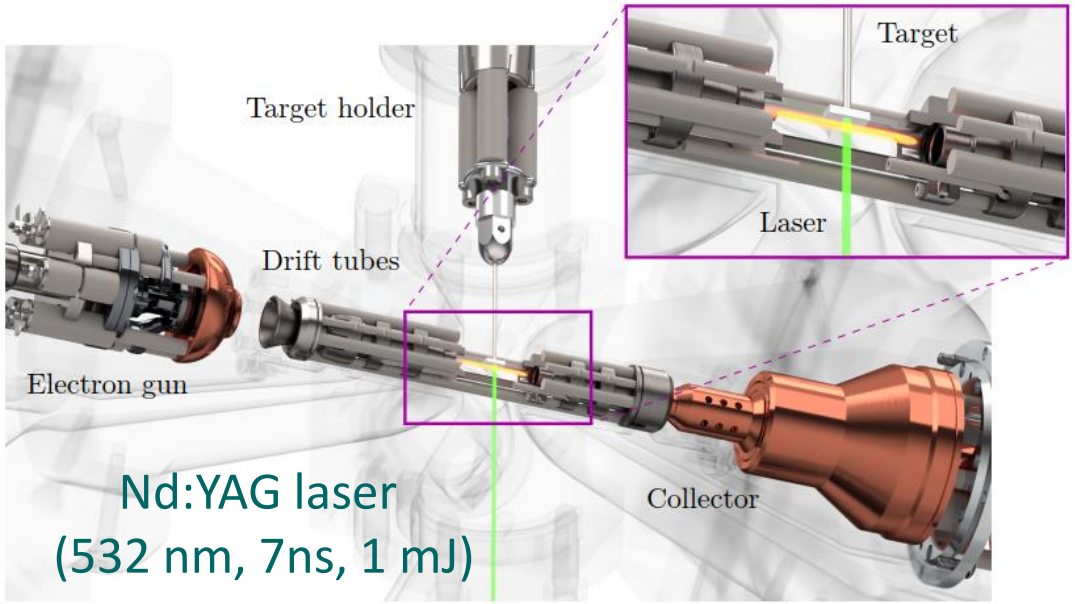

Nd:YAG laser
(532 nm, 7ns, 1 mJ)

Production of targets for PENTATRAP

PLA-target: a few mg of ^{163}Dy

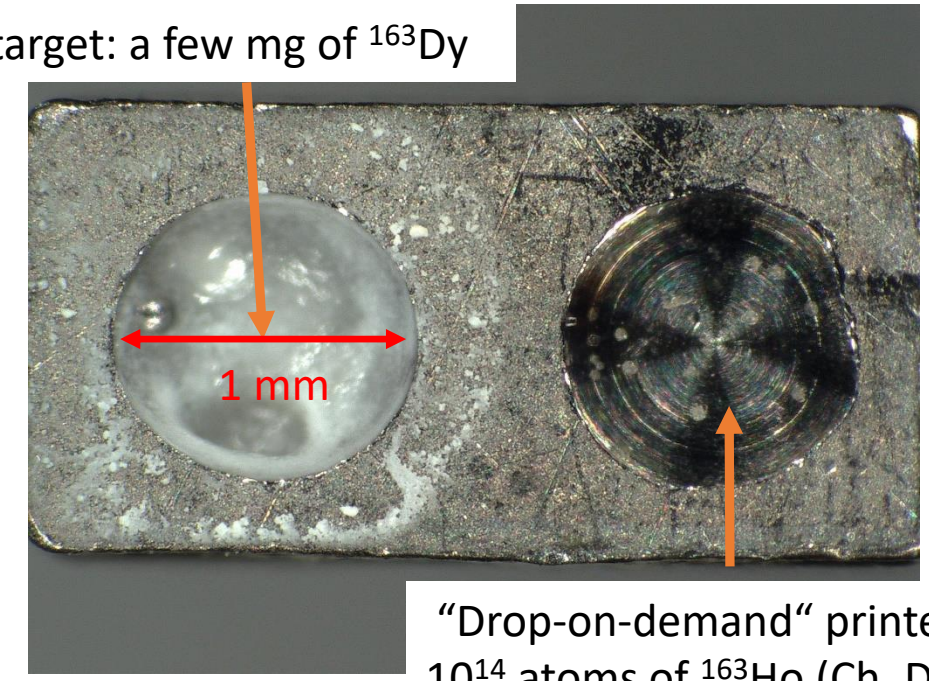

“Drop-on-demand“ printed target:
10^{14} atoms of ^{163}Ho (Ch. Düllmann)

Bradbury-Nielsen Gate: design

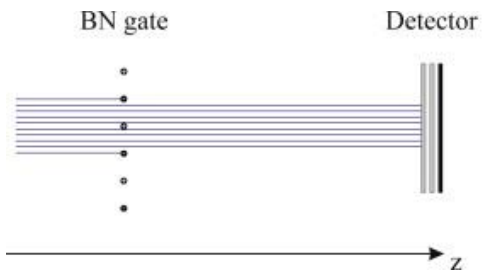

NO voltage applied

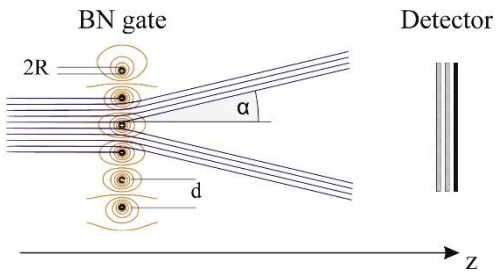

POS/NEG voltage applied

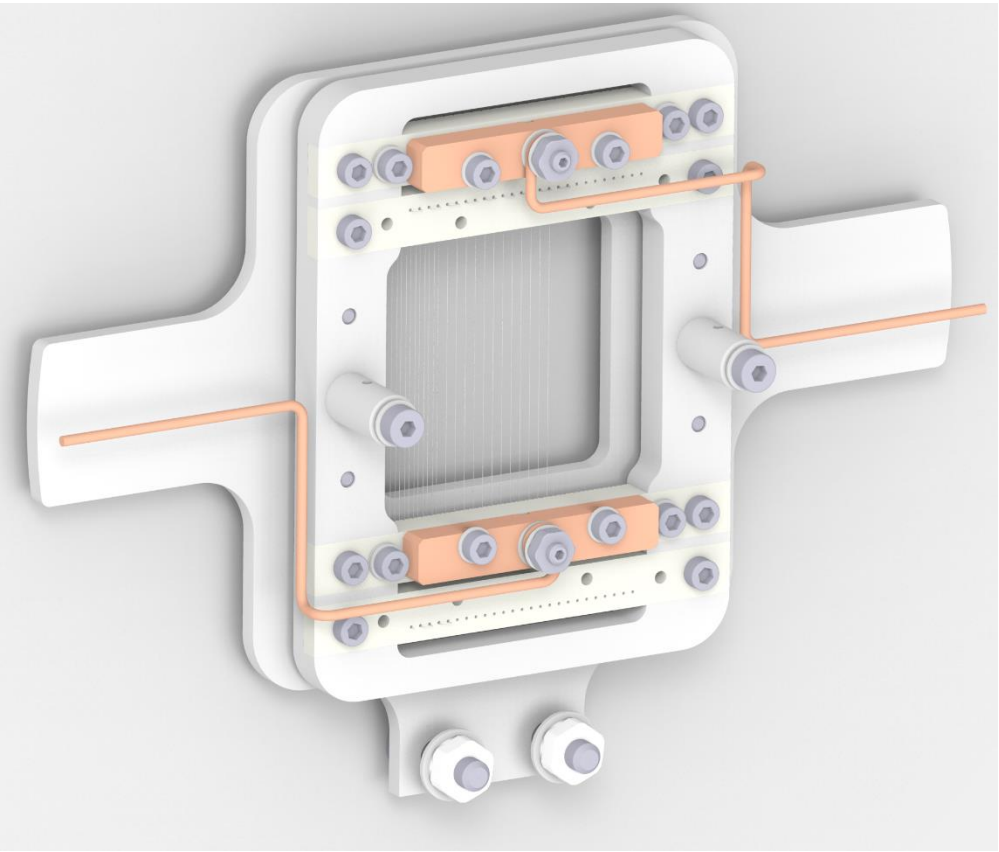

Wolf, R.N. et al., *NIMA 686*, 82 (2012)
Brunner, T. et al., *IJMS 309*, 97 (2012)

Bradbury-Nielsen Gate: performance

1st version: 40 ns pulse width/20-30 ns jitter

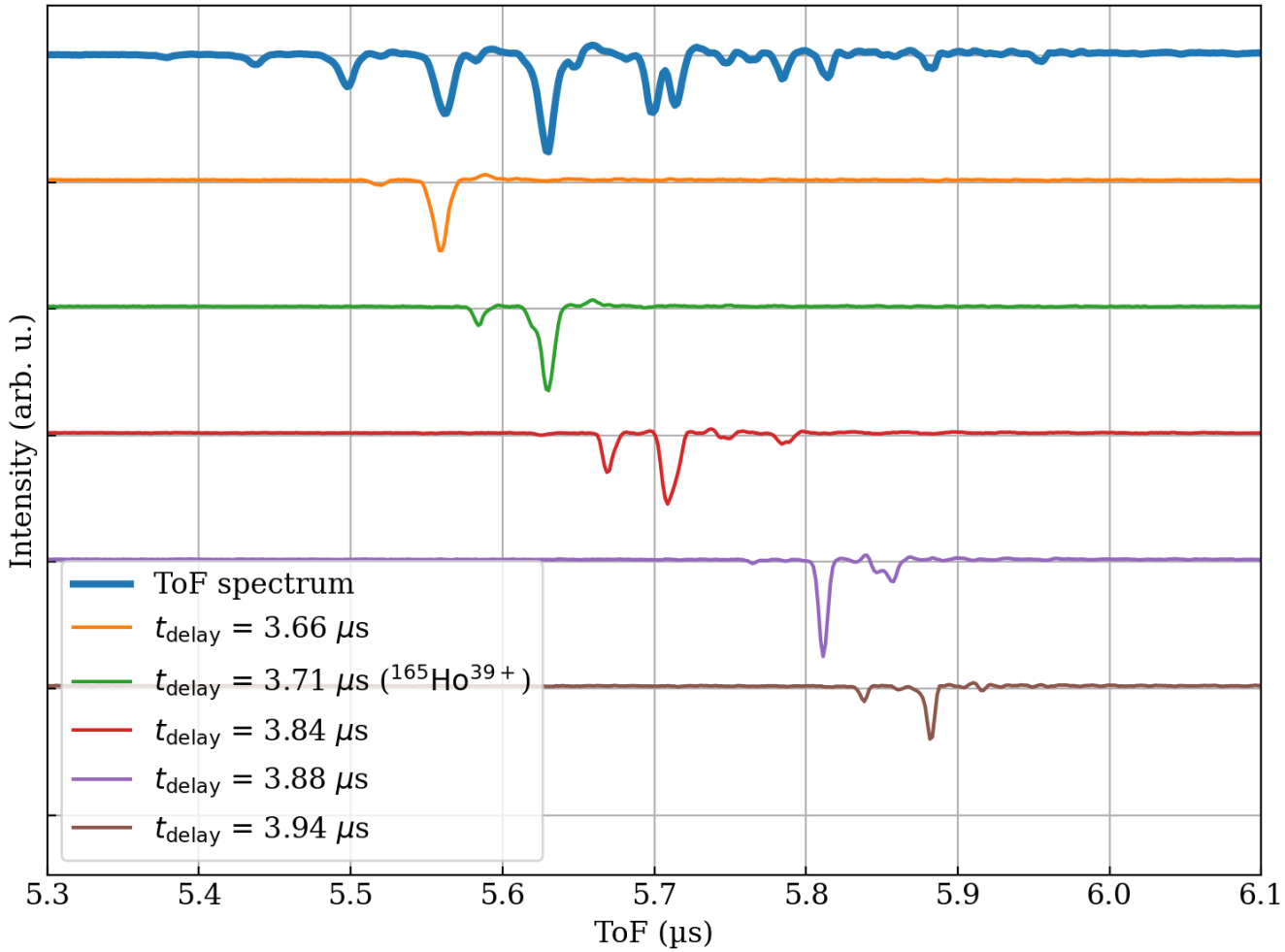

Bradbury-Nielsen Gate: performance

MOSFET switch for Bradbury-Nielsen Gate

- Switch based on two N-channel MOSFETs with gate drivers
- Pulse width reduced from 40 to 20 ns
- Near future: Faster MOSFETs placed inside the vacuum chamber

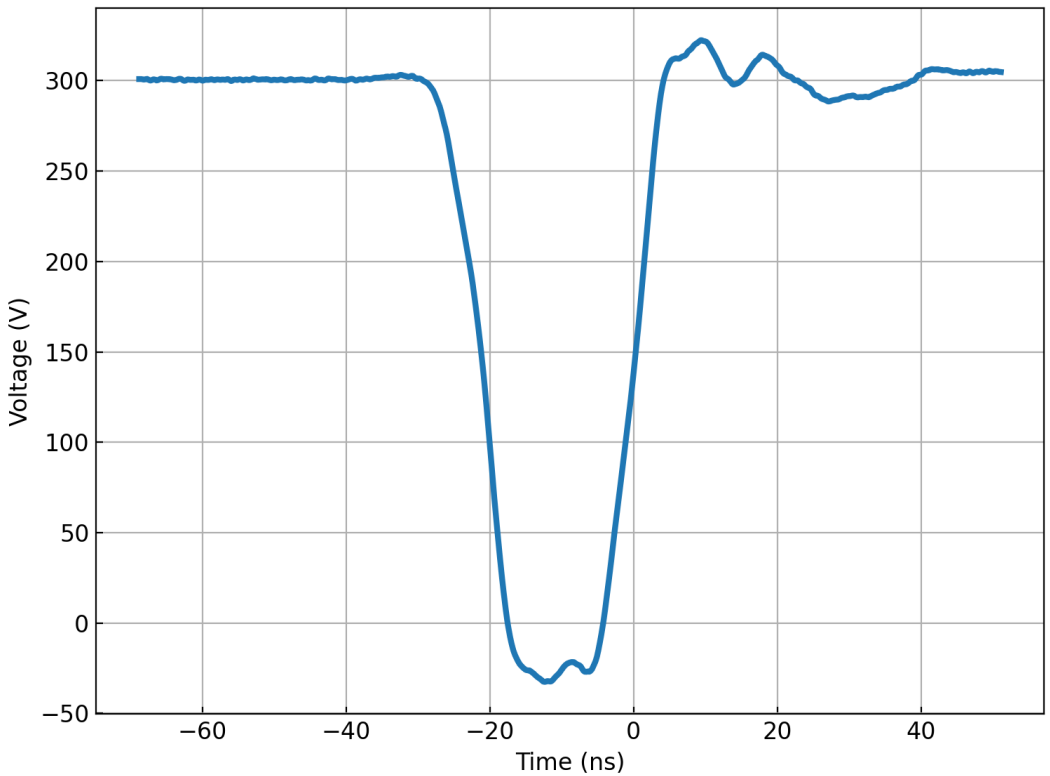

newest design ~20 ns pulse width

Measurement of trap frequencies with PENTATRAP

$$I_{ion}^{max} = 2\pi\nu_z q \frac{z_{max}}{D} = 15\ fA$$

$$z_{max} = 10\ \mu m$$

$$\nu_z = 500\ kHz$$

$$Re^{29+}$$

$$R_{LC} = 2\pi\nu_{LC} LQ = 25\ MOhm$$

$$L = 1.5\ mH$$

$$Q = 5000$$

$$U_{ion}^{max} = I_{ion}^{max} R_{LC} = 370\ nV$$

$$U_{th\_4K} = 70\ \mathrm{nV}$$

$$U_{th\_300K} = 600\ \mathrm{nV}$$

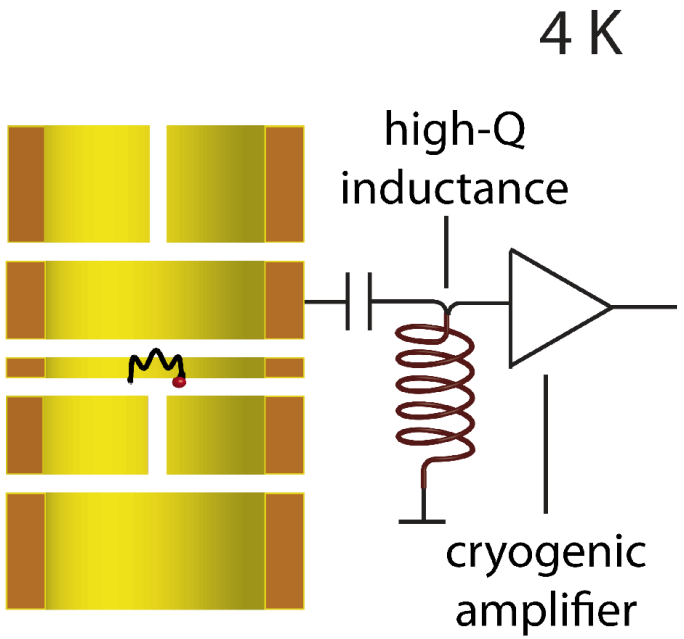

Measurement of trap frequencies with PENTATRAP

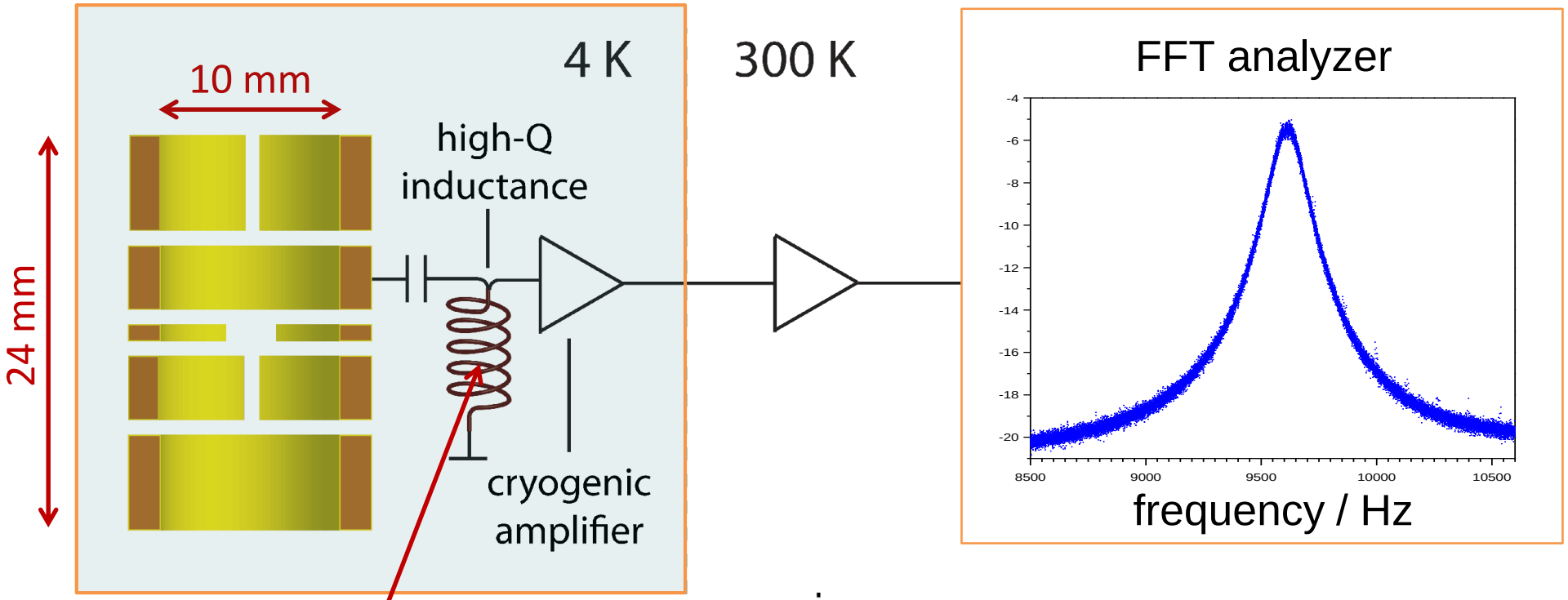

LC-circuit
(resonant circuit)

→

(1) thermal bath (4 K)
reduction of ion motional amplitudes

(2) frequency-measurement system

Measurement of trap frequencies with PENTATRAP

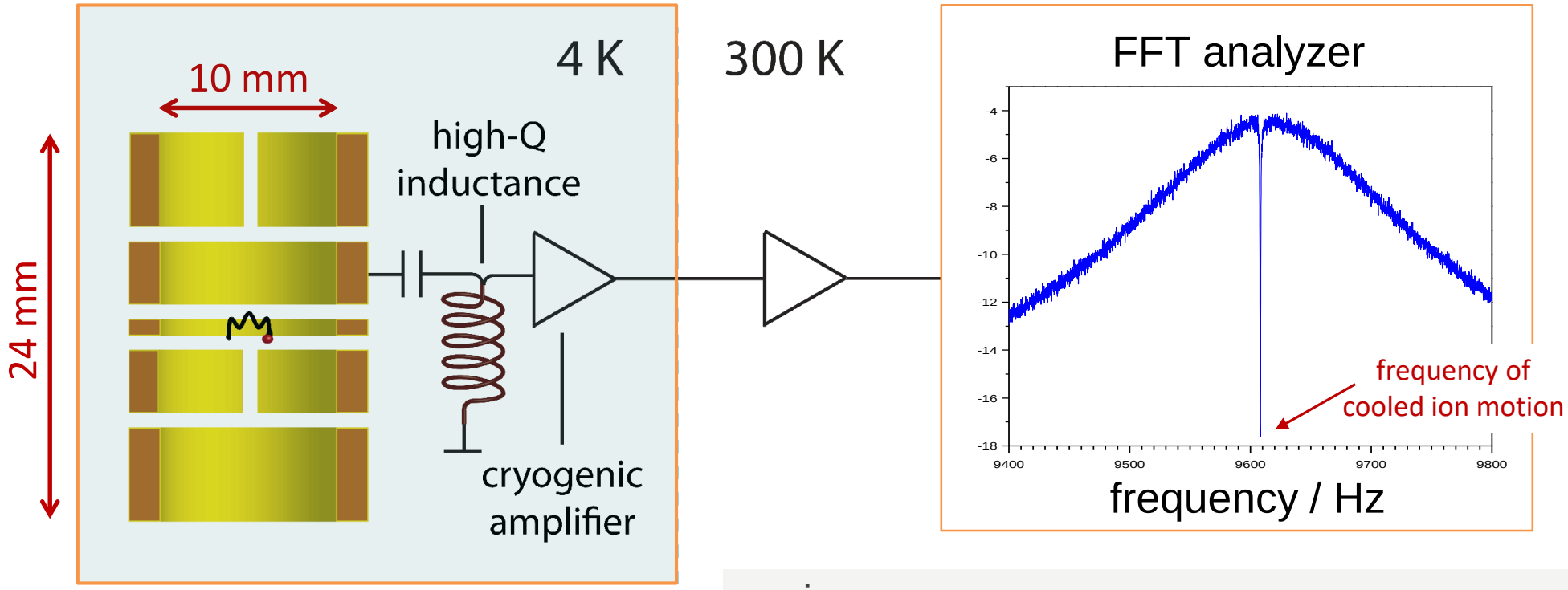

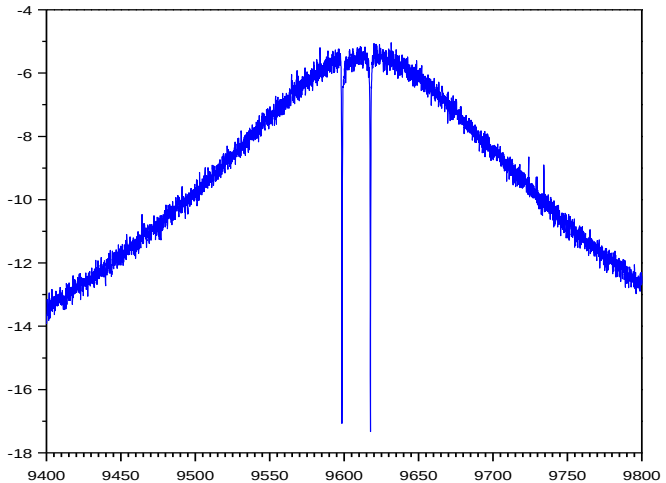

axial motion: $\nu_z = f\left(\frac{q}{m}U\right)$ $r_z \approx 10\ \mu m$

cyclotron motion: $\nu_+ \approx f\left(\frac{q}{m}B\right)$ $r_+ \approx 1\ \mu m$

magnetron motion: $\nu_- \approx f\left(\frac{U}{B}\right)$ $r_- \approx 1\ \mu m$

Penning Trap

$^{172}Yb^{42+}$

$\nu_c \approx \nu_+ \approx 26$ MHz
$\nu_z \approx 500$ kHz
$\nu_- \approx 4$ kHz

$$\nu_c^2 = \nu_+^2 + \nu_-^2 + \nu_z^2$$

$$\delta\nu_c = \sqrt{(\delta\nu_+)^2 + (2 \cdot 10^{-2}\delta\nu_z)^2 + (1.5 \cdot 10^{-4}\delta\nu_-)^2}$$

$$\frac{\delta\nu_c}{\nu_c} = 10^{-12} :$$

$\delta\nu_+ < 0.015\ mHz$	PnP technique
$\delta\nu_z < 1\ mHz$	dip technique
$\delta\nu_- < 100\ mHz$	double-dip technique

Measurement of trap frequencies with PENTATRAP

simultaneous measurement of ν_+ (**PnP**) and ν_z(**dip**)

D. J. Wineland and H. G. Dehmelt, J. of Appl. Phys. 46 (1975) 919

E. A. Cornell *et al.*, Phys. Rev. Letter 63 (1989) 1674

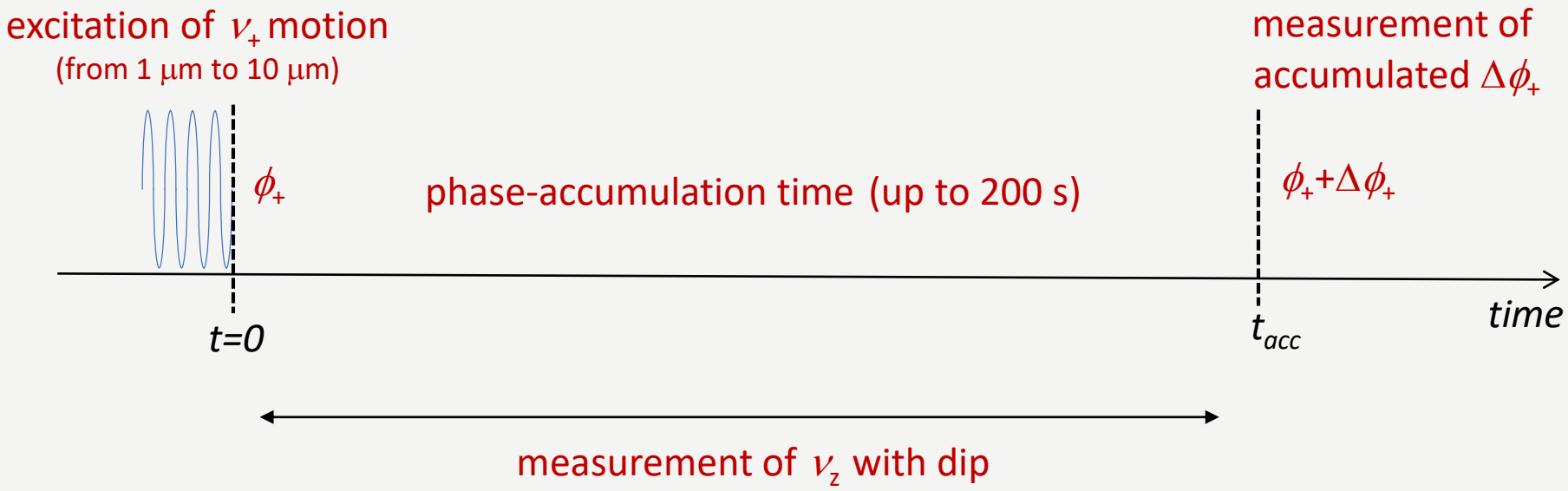

$$\nu_+ = \frac{\Delta\phi_+ + 2\pi N}{2\pi t_{acc}}$$

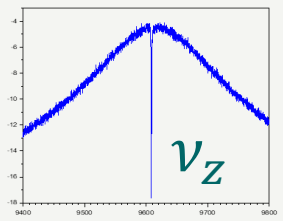

Determination of Q-value of β^- -decay of ^{187}Re

$$Q = M[^{187}\mathrm{Re}] - M[^{187}\mathrm{Os}] = M[^{187}\mathrm{Os}^{29+}]\cdot[R-1]+\Delta B$$

Maurits Haverkort
Heidelberg University Institute for Theoretical Physics
Zoltan Harman
Max-Planck Institute for Nuclear Physics
Paul Indelicato
Directeur de Recherche au CNRS

A multiconfiguration Dirac-Hartree-Fock method (MCDHF) ,
a fully relativistic approach, and its combination with Brillouin-Wigner many-body perturbation theory are used.

The ground state of the Re^{29+}ion is a simple Pd-like configuration $[Kr]4d^{10}\ {}^1S_0$,
the neutral Re atom is in the $[Xe]4f^{14}5d^5 6s^2\ {}^6S_{5/2}$ electronic state.

The Os ion and atom have an additional electron compared to their Re counterparts, thus their ground states are the Ag-like $[Kr]4d^{10}4f^2F_{5/2}$ and $[Xe]4f^{14}5d^6 6s^2\ {}^5D_4$ configurations, respectively.

Within the MCDHF scheme, the many-electron atomic state function is given as a linear combination of configuration state functions (CSFs) with a common total angular momentum (J), magnetic (M) and parity (P) quantum numbers: $|\Gamma PJM\rangle = \sum_k c_k |\gamma_k PJM\rangle$. The CSFs $|\gamma_k PJM\rangle$ are constructed as jj-coupled Slater determinants of one-electron orbitals, and γ_k summarizes all the information needed to fully define the CSF, i.e. the orbital occupation and coupling of single-electron angular momenta. Γ collectively denotes all the γ_k included in the representation of the ground state.

The GRASP2018 code package [30] is used.

ECHo Experiment

^{163}Ho wire preparation

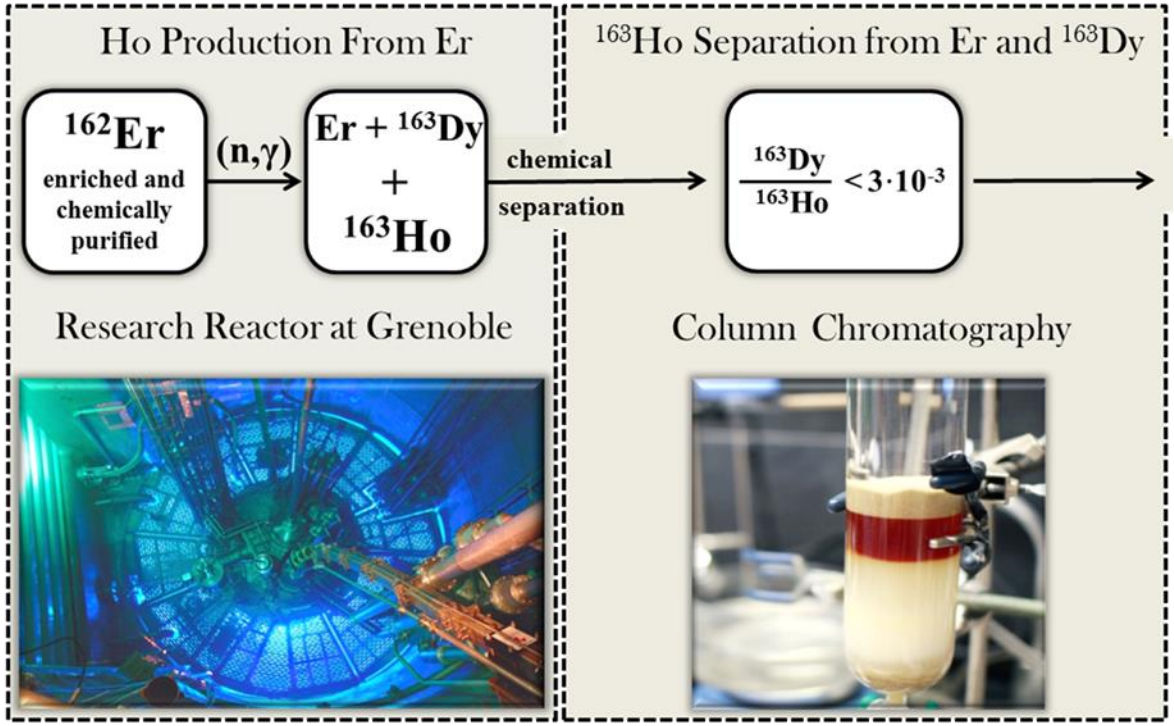

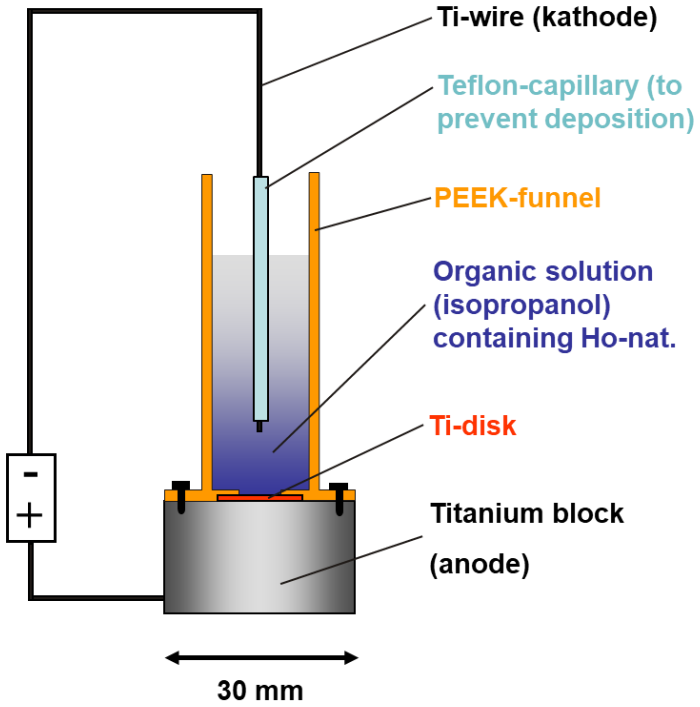

atomic metastable states in Re^{29+} and Os^{30+}

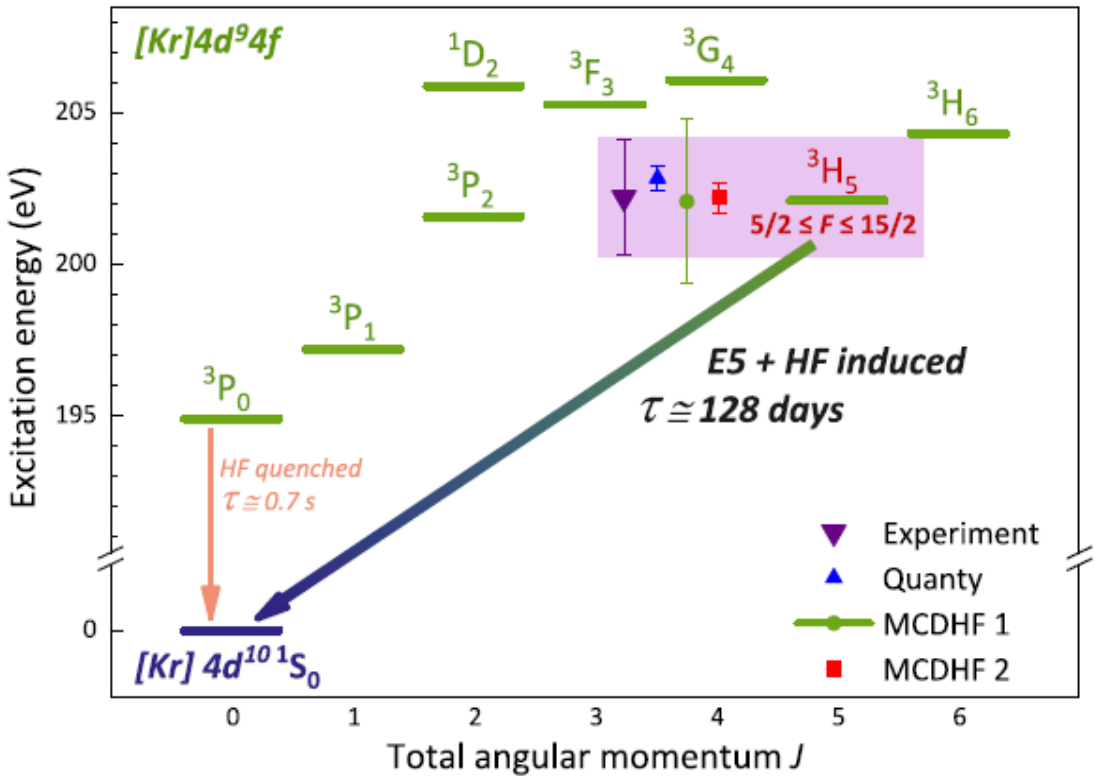

Figure 2: The $4d^{10}$ ground state and relevant $4d^9 4f$ excited electronic states of the $^{187}Re^{29+}$ ion. Comparison of the experimental result and theoretical values obtained using multi-configuration Dirac-Hartree Fock approaches in two different implementations (MCDHF 1 and 2) and by means of a configuration-interaction (Quanty) calculation is shown in the coloured bar.

$^{20}Ne^{10+}$ vs $^{12}C^{6+}$

light non-mass doublet

$$R \equiv \frac{\nu_c(Ne)}{\nu_c(C)} = Function\left(\frac{\rho_+(Ne)-\rho_+(C)}{\rho_+}\right)$$

R was measured at several ρ_+ values

extrapolation to $\rho_+ = 0$

$$\delta R_{\rho_+ = 0} \approx 10^{-11}$$

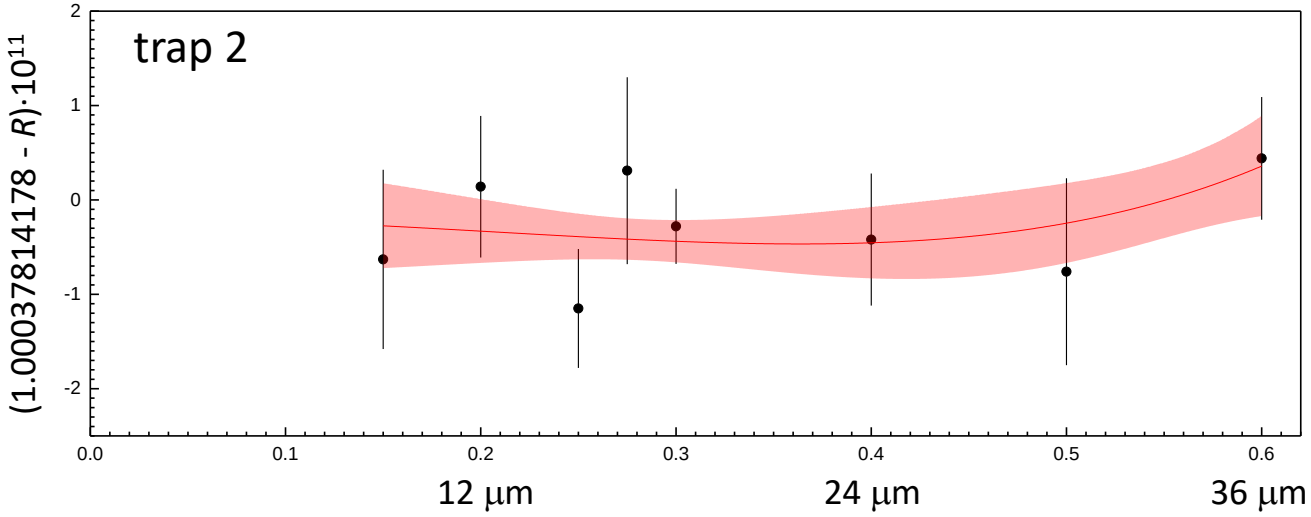

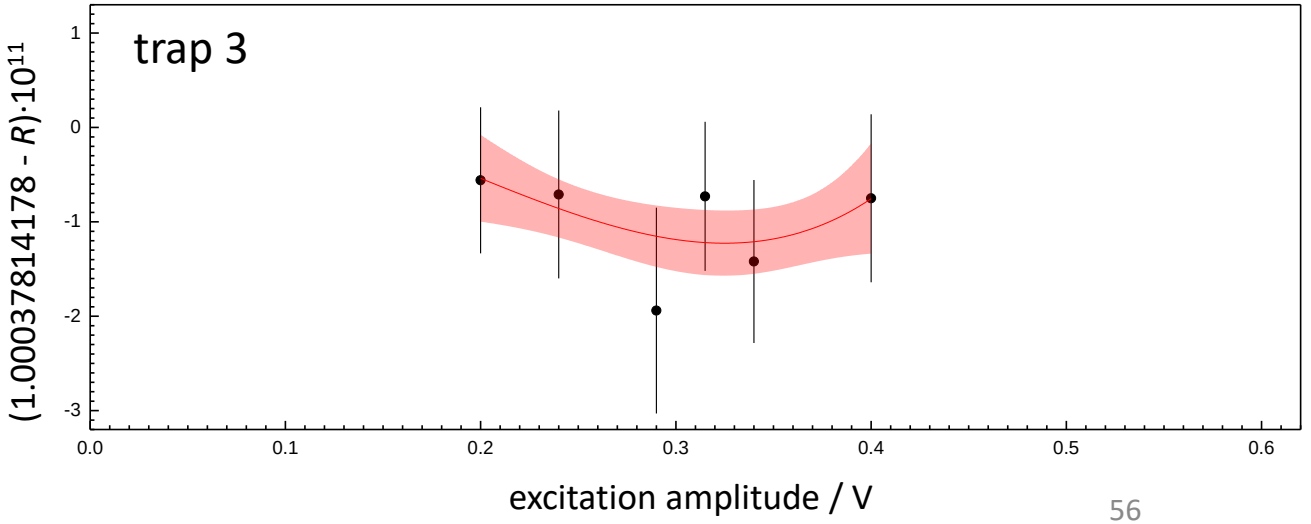

		$\delta m / m$	Penning-trap Group	Year
√	20Ne	7.5E-11	MIT / DiFilippo / Pritchard	1995
	14N	1.7E-11	MIT / DiFilippo / Pritchard	1995
	16O	2.0E-11	UW / van Dyke	2006
	28Si	2.0E-11	FSU / Redshaw / Myers	2008

↑

We are planning to measure other low masses sooner or later

dark matter and 5th force

$$\Delta\nu_i = C_1 \cdot \frac{m_1 - m_2}{m_1 m_2} + C_2 \cdot \Delta\nu_j + \text{[higher−order SM effects + LDM bosons]}$$

$$\nu_i(\text{isotope}_1) - \nu_i(\text{isotope}_2) \equiv \Delta\nu_i$$

King plot

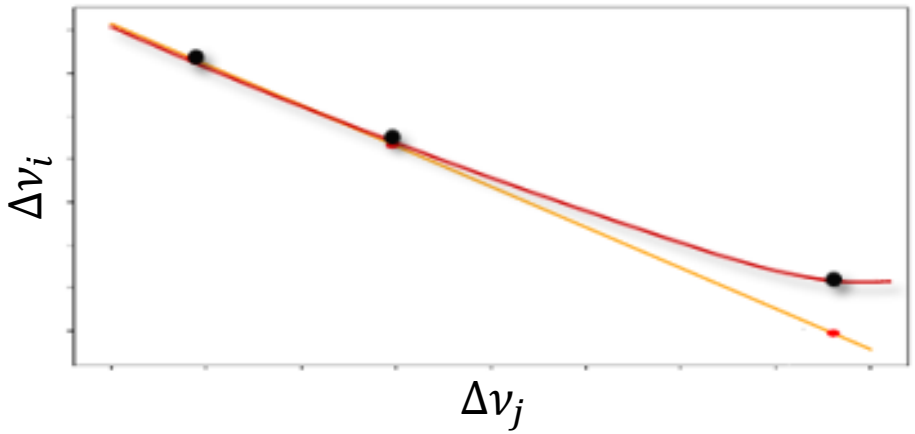

one needs elements with many even-even isotopes
and quadrupole (narrow optical) transitions:

^{168,170,172,174,176}Yb	$^2S_{1/2} \leftrightarrow {}^2D_{5/2}$ (411 nm) $^2S_{1/2} \leftrightarrow {}^2D_{3/2}$ (436 nm) $^2S_{1/2} \leftrightarrow {}^2F_{7/2}$ (467 nm)	I. Counts et al., PRL 125, 123002 (2020) J. Hur et al., arXiv: 2201.03578 (2022)
^{40,42,44,46,48}Ca	$4s^2S_{1/2} \leftrightarrow 3d^2D_{5/2}$ (729 nm) $4s^2S_{1/2} \leftrightarrow 3d^2D_{3/2}$ (732 nm)	C. Solaro et al., PRL 125, 123003 (2020) F.W. Knollmann et al., PRA 100, 022514 (2019)
^{84,86,88,90}Sr	$5S_{1/2} - 4D_{5/2}$ $1S_0 - 3P_1$, $1S_0 - 3P_0$	T. Manowitz et al., PRL 123, 203001 (2019) H. Miyake et al., PRR 1, 033113 (2019)

FUTURE:

$$\delta(\Delta\nu_i) \approx 10 \text{ mHz}$$

$$\delta\left(\frac{m_1}{m_2}\right) \approx 5 \cdot 10^{-12}$$

dark matter and 5th force

^{168,170,172,174,176}Yb

I. Counts et al., PRL 125, 123002 (2020) (MIT, USA)

Measurement: two quadrupole transitions in 5 Yb^+ Isotopes, $6s^2S_{1/2} \leftrightarrow 5d^2D_{5/2}$ (411 nm), $6s^2S_{1/2} \leftrightarrow 5d^2D_{3/2}$ (436 nm)

with an uncertainty of 300 Hz (limited by laser drift).

Method: ion in Paul trap; Doppler cooled on $6s^2S_{1/2} \rightarrow 6p^2P_{1/2}$ to 0.5 mK; coherent Ramsey spect./electron-shelving scheme.

Results: King plot shows a $3 \cdot 10^{-7}$ deviation from linearity at 3σ uncertainty level.

Indication of the fifth force or higher order nuclear effects within the SM.

Outlook: (statement in the paper)

In the future, the measurement precision can be increased by several orders of magnitude by cotrapping two isotopes. This improvement, also in combination with measurements on additional transitions, such as the $^2S_{1/2} \rightarrow {}^2F_{7/2}$ octupole transition in Yb^+ or
clock transitions in neutral Yb, will allow one to discriminate between nonlinearities of different origin.

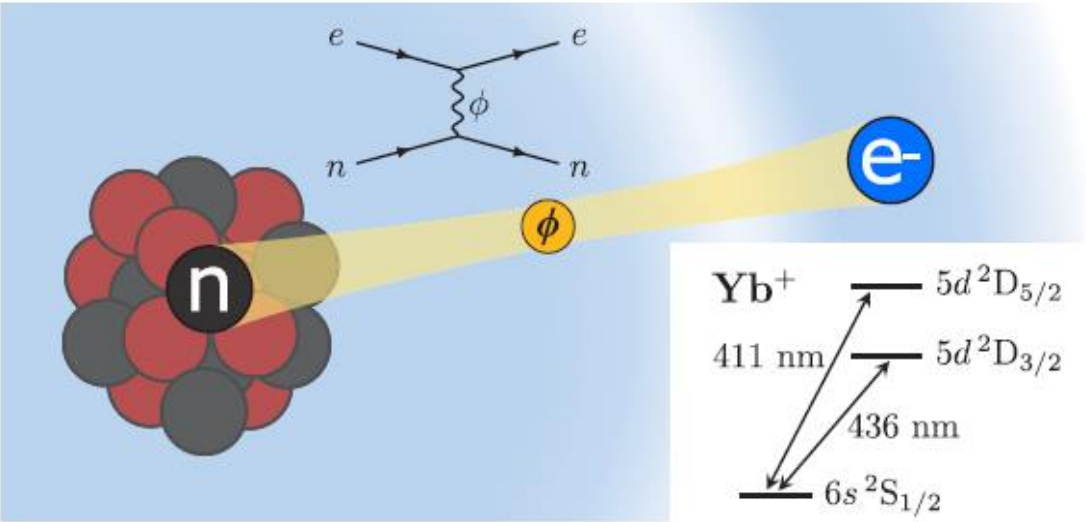

taken from the paper

dark matter and 5th force

^{168,170,172,174,176}Yb

I. Counts et al., PRL 125, 123002 (2020) (MIT, USA)

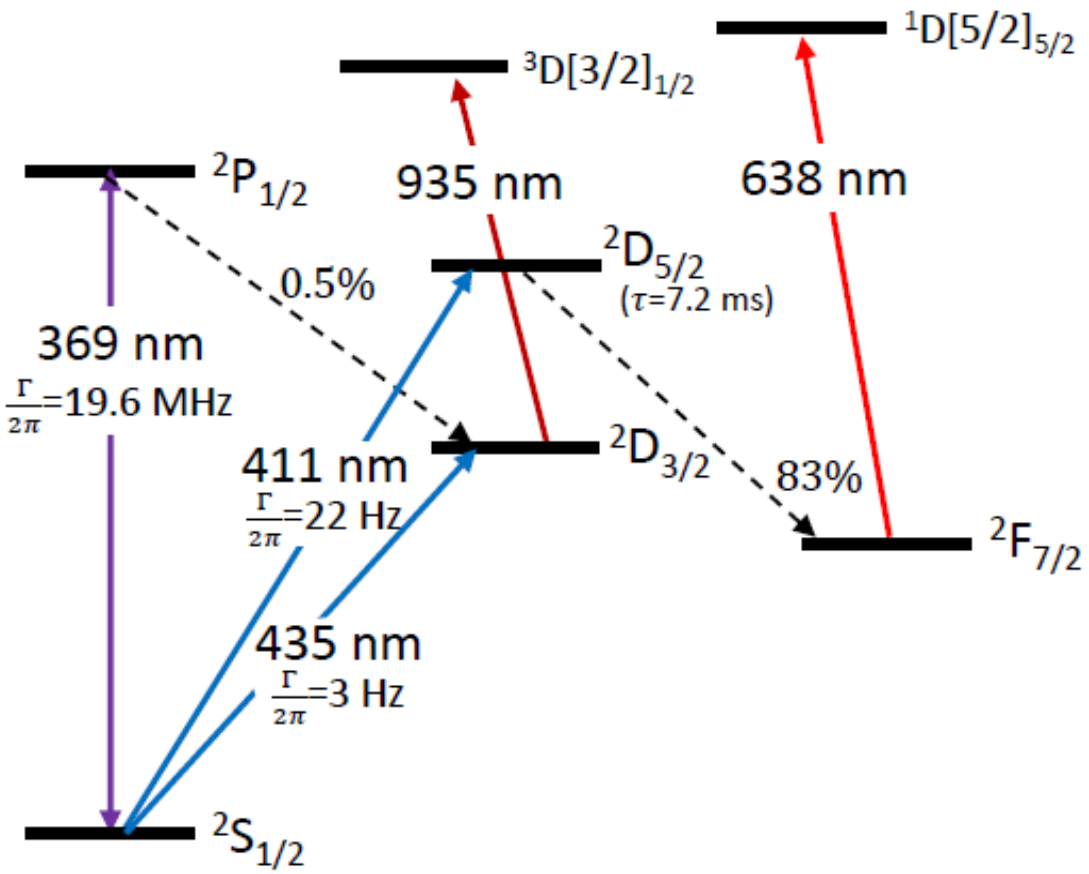

FIG. S1. Partial Yb^+ level diagram.

taken from the paper

dark matter and 5th force

$^{40,42,44,46,48}Ca$

C. Solaro et al., PRL 125, 123003 (2020) (Aarhus University, Denmark)

F.W. Knollmann et al., PRA 100, 022514 (2019) (Williams College, USA)

Measurement: two quadrupole transitions in 5 Ca^+ Isotopes, $4s^2S_{1/2} \leftrightarrow 3d^2D_{5/2}$ (729 nm) , $4s^2S_{1/2} \leftrightarrow 3d^2D_{3/2}$ (732 nm)

with an uncertainty of 20 Hz.

Method: (1) frequency-comb Raman spectroscopy on $3d^2D_{3/2} \leftrightarrow 3d^2D_{5/2}$ (C. Solaro et al.)

(2) co-trapped ions in a Paul trap, laser spectroscopy on $4s^2S_{1/2} \leftrightarrow 3d^2D_{5/2}$ (729 nm) (F.W. Knollmann et al.)

Results: no non-linearity of the King's plot is observed.

Outlook:

D-D transitions with 10 mHz accuracy, S-D with 1 Hz.

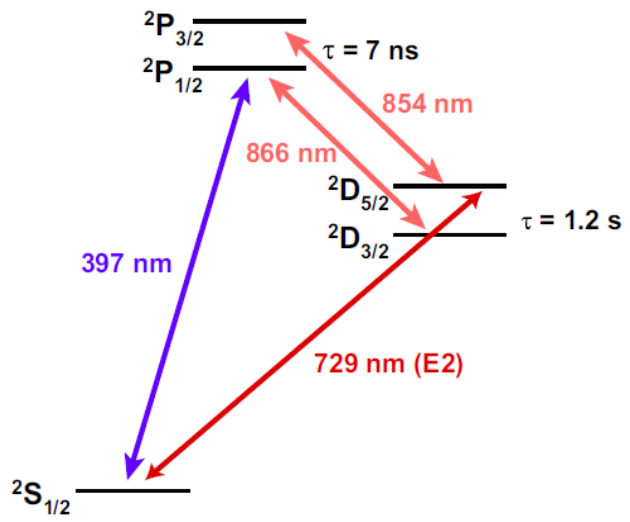

FIG. 1. Level diagram for nuclear spin-zero isotopes of Ca^+, with natural lifetimes listed. The 397-nm transition is used for Doppler cooling and fluorescence detection, while metastable $^2D_{3/2,5/2}$ levels are repumped by transitions at 866 and 854 nm, respectively.

taken from the paper by F.W. Knollmann

Raman spectroscopy

A Raman transition couples two atomic levels by the absorption of a photon from one Raman beam (pump beam) and by stimulated emission of another one into the other beam (Stokes beam).

The narrow linewidth of Raman transitions can be used to resolve atomic motional sidebands.

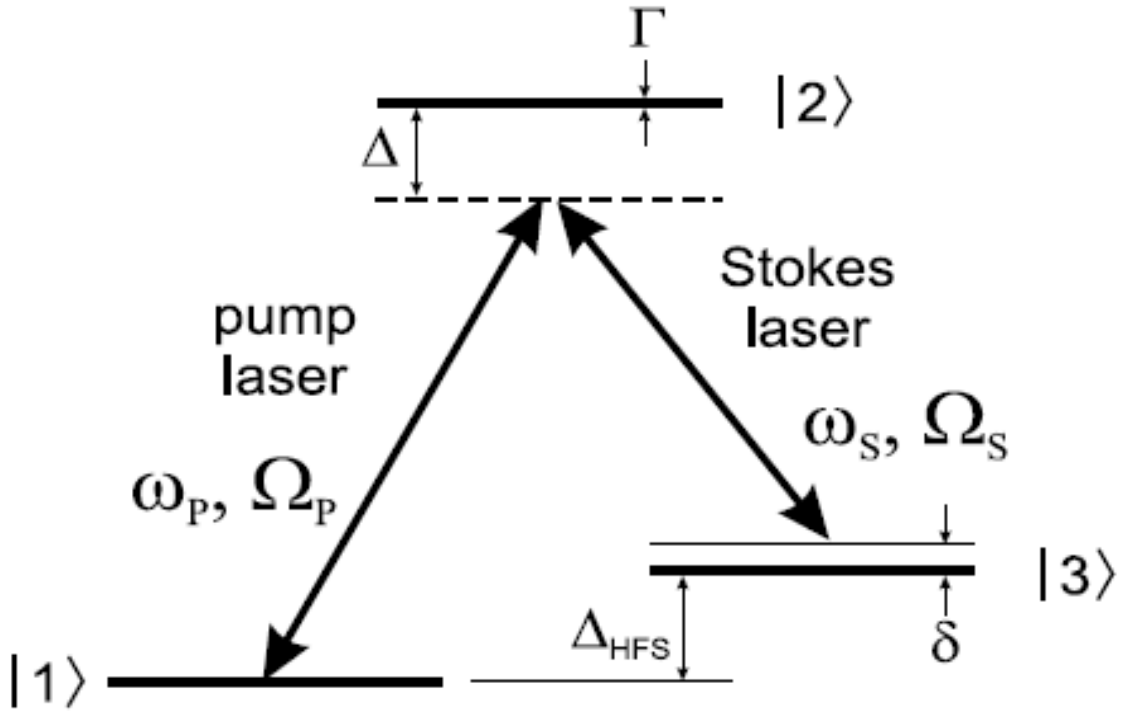

dark matter and 5th force

$^{84,86,87,88,90}Sr$

T. Manowitz et al., PRL 123, 203001 (2019) (Weizmann Institute of Science, Israel)

H. Miyake et al., PRR 1, 033113 (2019) (Joint Quantum Institute, USA)

Measurement: (1) $^1S_0 - {}^3P_1$ (689 nm, linewidth=7.4 kHz), $^1S_0 - {}^3P_0$ (698 nm, linewidth= mHz), with an uncertainty of a few kHz.

(2) electric quadrupole (0.4 Hz) $^5S_{1/2} - {}^4D_{5/2}$ with an uncertainty of 9 mHz.

Method: (1) laser spectroscopy in optical dipole trap.

(2) decoherence free subspaces (DFSs). Direct probe of the isotope shift with 9 mHz uncertainty.

Results: nonlinearity in the measured values. The problem may be ^{87}Sr (center of hyperfine splitting is determined wrongly).

^{90}Sr is needed (radioactive, 29 years life time).

Outlook:

Method of decoherence free subspaces with all isotopes.

dark matter and 5th force

^{130,132,134,136,138}Ba

P. Imgram et al., PRA 99, 012511 (2019) (TU Darmstadt, Germany)

Measurement: $6s^2S_{1/2} - 6p^2P_{1/2}$ (D1, 493 nm), $6s^2S_{1/2} - 6p^2P_{3/2}$ (D2, 455 nm), with accuracy of 200 kHz.

Method: collinear/anticollinear laser spectroscopy on collimated fast ion beams.

Results: uncertainty comparable to ion trap measurements on dipole transitions but far from the needed one for 5th force.

^{142,144,146,148,150}Nd

N. Bhatt et al., ArXiv 2002.08290 (Uni of Toronto, Canada)

Measurement: $4f^46s$ - $[25044.7]_{7/2}$ (399 nm), $4f^46s$ - $[25138.6]_{7/2}$ (397 nm) with accuracy of a few 100 kHz.
Method: laser absorption spectroscopy of cold ions in a neutral plasma.

Results: uncertainty comparable to ion trap measurements on dipole transitions but far from the needed one for 5th force.

Outlook:

several telecommunication forbidden transitions 1500 nm with sub-Hz uncertainty.

Stabilization of LHe level and He pressure

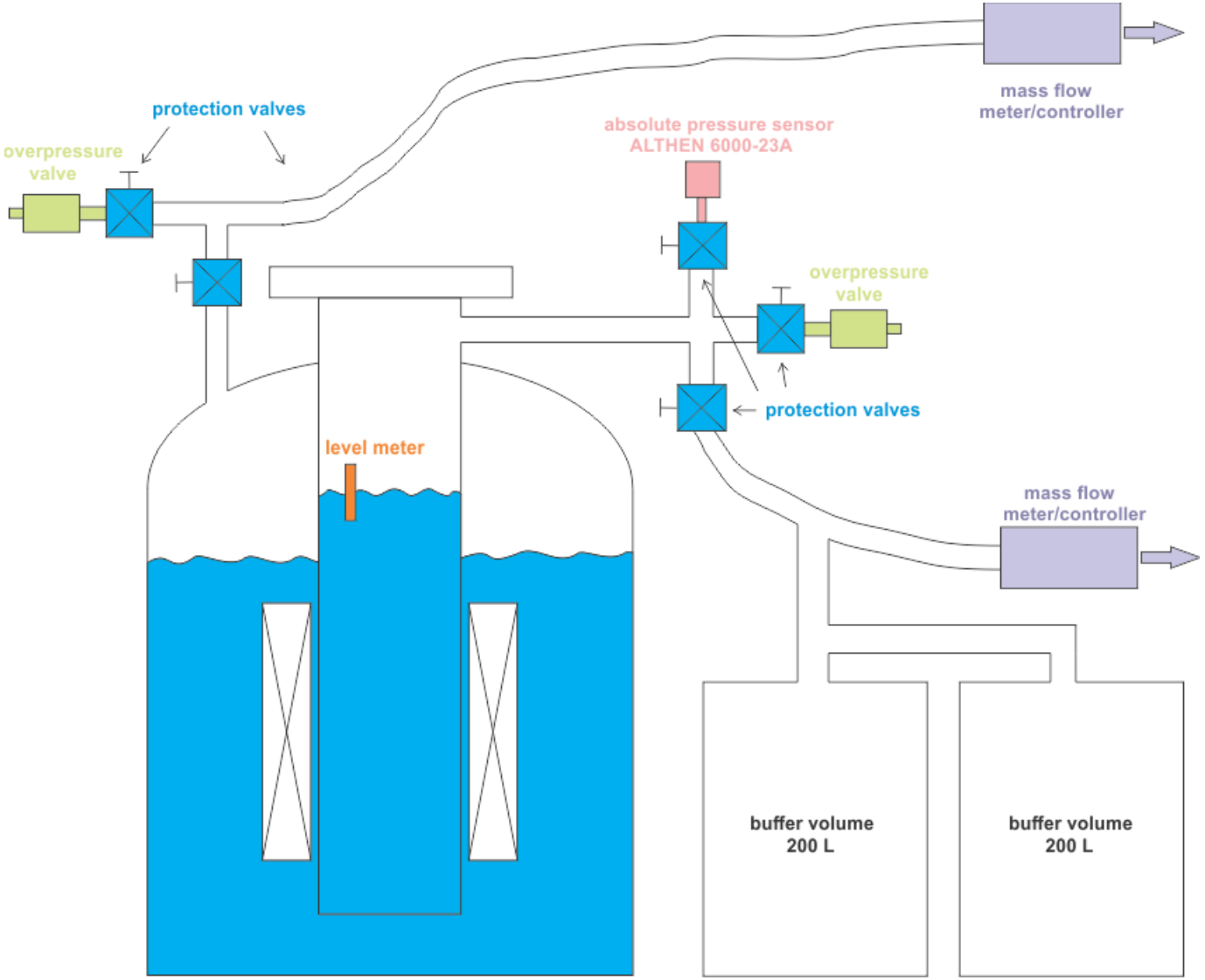

Stabilization of LHe level and He pressure

Series 1000, 6000 & 9000
Intelligent Transmitters

ALTHEN SENSORS & CONTROLS

bar

SERIES 1000, 6000 & 9000
Intelligent Transmitters

Intelligent Transmitters consist of a Digiquartz® Pressure Transducer and a digital interface board in an integral package. Commands and data requests are sent via two-way RS-232 or RS-485 serial interfaces. Direct digital outputs in engineering units are provided with parts-perbillion resolution using the built-in, anti-aliasing IIR filter mode. Typical accuracy is 0.01% even under harsh environmental conditions. All intelligent transmitters are preprogrammed with calibration coefficients for full plug-in interchangeability.

LOW-ΔP-FLOW
Massedurchflussmesser/-regler
mit geringem Druckabfall und für korrosive Gase

> Einführung
Bronkhorst High-Tech B.V. ist europäischer Marktführer für thermische Massedurchflussmesser/-regler und elektronische Druckregler. Mit mehr als 35 Jahren Erfahrung in der Entwicklung und Fertigung präziser und zuverlässiger Sensoren und Regler für Gase und Flüssigkeiten bietet Bronkhorst innovative Lösungen für eine Vielfalt unterschiedlichster Anwendungen. Bronkhorst liefert für die verschiedensten Märkte für Labor und Industrie eine Anzahl von Standardausführungen wie auch individuell kundenspezifisch entwickelte Instrumente.

> Geringem Druckabfall und für korrosive Gase geeignet
In vielen Anwendungsbereichen stehen zur Messung und Regelung von Gasströmen nur geringe Druckdifferenzen

Polynomial Method

Ann. Inst. Statist. Math.
30 (1978), Part A, 9-14

A BAYESIAN ANALYSIS OF THE MINIMUM AIC PROCEDURE

HIROTUGU AKAIKE

(Received Oct. 15, 1977; revised Apr. 24, 1978)

Summary

By using a simple example a minimax type optimality of the minimum AIC procedure for the selection of models is demonstrated.

Biometrika (1989), **76**, 2, *pp.* 297–307
Printed in Great Britain

Regression and time series model selection in small samples

BY CLIFFORD M. HURVICH
Department of Statistics and Operations Research, New York University, New York NY 10003, U.S.A.

AND CHIH-LING TSAI
Division of Statistics, University of California, Davis, California 95616, U.S.A.

SUMMARY

A bias correction to the Akaike information criterion, AIC, is derived for regression and autoregressive time series models. The correction is of particular use when the sample size is small, or when the number of fitted parameters is a moderate to large fraction of the sample size. The corrected method, called AIC_C, is asymptotically efficient if the true model is infinite dimensional. Furthermore, when the true model is of finite dimension, AIC_C is found to provide better model order choices than any other asymptotically efficient method. Applications to nonstationary autoregressive and mixed autoregressive moving average time series models are also discussed.

some photos of traps and axial resonators

trap tower

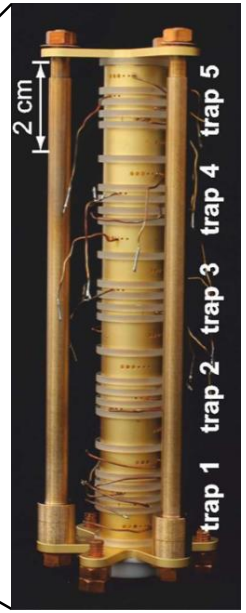

trap electrodes

NbTi toroidal coil

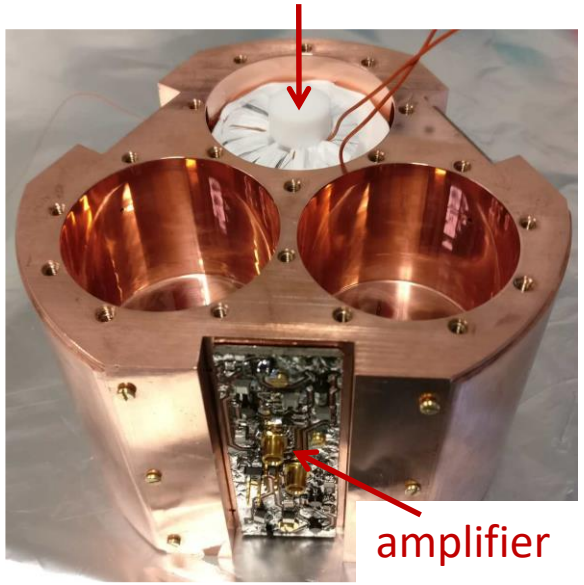

amplifier

^{163}Ho EC decay spectrum

M. Braß and M.W. Haverkort, “Ab initio calculation of the electron capture spectrum of ^{163}Ho: Auger-Meitner decay into continuum states”, arxiv: 2002.05989v1

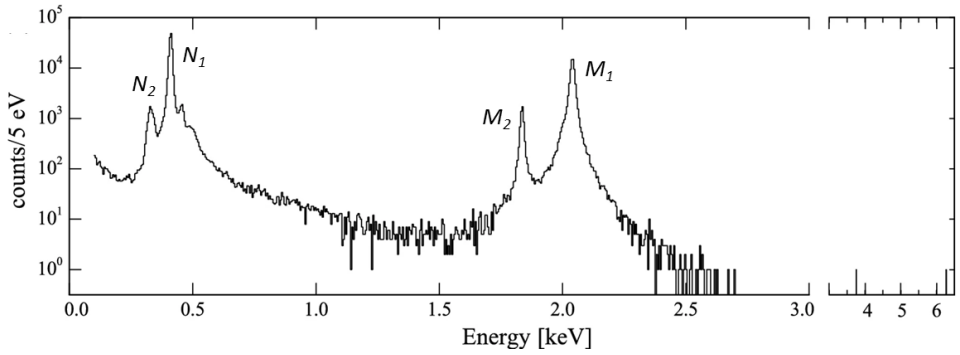

Calculation Method: core level x-ray spectroscopy

De-excitation is driven by Coulomb interactions between the remaining electrons

Spectrum is a contribution of single and multiple electronic holes.

Mainly Auger-Meitner mechanism (electrons).

Interaction of gold valence electrons with Ho electrons.

Fano effect – interference between different channels that reach the same final state.

a Fano resonance is a type of resonant scattering phenomenon that gives rise to an asymmetric line-shape.

The Fano resonance line-shape is due to interference between two scattering amplitudes, one due to scattering within a continuum of states (the background process) and the second due to an excitation of a discrete state (the resonant process).

Systematics

parameter	trap2	(err)	trap3	(err)
d4	8.878e-4	26	7.290e-4	80
TR@C4=0	0.880143	4	0.880331	10
d6	-6.1e-5	4	-1.1e-5	1.5
TR@C6=0	0.87860	13	0.8797	12
B0	7.002766410	10	7.002774823	10
B1 uT/mm	1.41	27	-1.49	16
B2 uT/mm2	6.4e-2	5	2.2e-2	5
Temp resonator	4.6	0.5	11.5	1.6
pnp excitation radius	17	3	21	3

5th force

Mass situation

Nuclide	Current mass precision (AME2016) $\delta m/m$	Labs performing spectroscopy measurements of the IS	Needed relative precision compared to IS precision, a factor of roughly: $\frac{m_A}{m_{A_0} - m_A}$	Current IS precision	Needed mass precision
Ca40	**5.51e-10**	PTB (Germany) IQOQI (Austria)			
Ca42	**3.79e-09**				
Ca44	**7.92e-09**		48/8 = 6	~ 1e-08	~ 2e-09
Ca46	**5.22e-08**				
Ca48	**2.15e-09**				
Sr84	**1.59e-08**	Weizmann Institute (Israel) RIKEN (Japan)			
Sr86	6.53e-11		88/4 = 22	~ /	
Sr88	6.81e-11				
Sr90	**2.54e-08**				
Yb168	**7.63e-09**	Weizmann Institute (Israel) MIT (USA) Kyoto (Japan)			
Yb170	6.47e-11		176/8 = 22	~ 1e-07	~ 5e-09
Yb172	8.14e-11				
Yb174	6.32e-11				
Yb176	8.53e-11				